Journal of Manufacturing Processes 84 (2022) 1001–1029

Contents lists available at ScienceDirect

Journal of Manufacturing Processes

journal homepage: www.elsevier.com/locate/manpro

Review

An overview of modern metal additive manufacturing technology

Mark Armstrong *, Hamid Mehrabi, Nida Naveed

Faculty of Technology, School of Engineering, University of Sunderland, Sunderland SR1 3SD, UK

ARTICLE INFO

Keywords:
Metal additive manufacturing
Additive manufacturing technology
Additive manufacturing processes
Rapid prototyping
Manufacturing process

ABSTRACT

There has been significant development in metal additive manufacturing (MAM) technology over the past few decades, and considerable progress has been made in understanding how various processes and their parameters influence the properties of printed metallic parts. Despite this, the knowledge concerning its characteristics has been dispersed across a variety of publications and sources, making it difficult to gain a comprehensive understanding of the entire field, especially for businesses interested in additive manufacturing (AM). In order to bridge this gap, periodic reviews encompassing state-of-the-art as the whole are necessary. Therefore, this article provides a comprehensive overview of the essential features of MAM techniques based on the most recent scientific knowledge. It explores emerging research on four of the most significant technologies, including material extrusion (ME), binder jetting (BJ), powder bed fusion (PBF), and directed energy deposition (DED). As well as providing an outline of fundamental process characteristics, ongoing efforts to optimize them and current challenges, it also highlights gaps in understanding and future research and development needs. A significant feature of this review is the provision of substantial documentation regarding the mechanical properties of materials processed by a variety of commercial systems, including a variety of novel hybrid additive manufacturing (HAM) machines. This is accompanied by an investigation into the most recent works done to characterize the environmental impact along with a conceptual framework for improving the energy efficiency (EE) of the manufacturing process. As a result of reporting on both the characteristics of several MAM processes along with their sustainability features in one integrated article, it is anticipated that this information will serve as a valuable resource for both the academic and manufacturing communities to better appreciate and understand what differentiates MAM from traditional manufacturing (TM) processes, thus facilitating its future advancement and adoption.

1. Introduction

Manufacturing processes are in the midst of a paradigm shift - one that integrates the growing trend of fabricating more sophisticated products alongside the emergence of advanced manufacturing technologies, often referred to as Industry 4.0 (I4.0) or more commonly known as the fourth industrial revolution [1]. Underpinning one of the five I4.0 central research themes is a group of technologies that have emerged from a process that was originally known as rapid prototyping (RP), developed in the 1980s [2]. As this technology matured over the years through significant advances in materials science along with hardware and software developments, industry and academia realized that the term RP no longer accurately reflected the true capabilities of modern technologies. The latest machines could manufacture functional parts with material properties comparable to those fabricated traditionally, especially for metals [3]. Instead of subtracting or forming material into the shape of a product, feedstock in the form of wire or powder could be either fused, melted, or bonded layer by layer directly from a three-dimensional (3D) computer-aided design (CAD) file and with minimal human intervention [4]. Over the course of this period, several terms and definitions were introduced that were frequently ambiguous and confusing, and it became evident that these would need to be standardized. Through cooperation between the American Society for Testing and Materials (ASTM) and the International Standards Organisation (ISO), 52,900:2017 [5] was developed, establishing additive manufacturing (AM) as the official industry name while recognizing 3D printing as a commonly used synonym.

Today, modern AM technologies can be used to manufacture products from various materials, such as metals, polymers, ceramics, and

* Corresponding author at: The Faculty of Technology, School of Engineering, The University of Sunderland, Edinburgh Building, City Campus, Chester Road, Sunderland SR1 3SD, UK.
E-mail addresses: mark.armstrong@research.sunderland.ac.uk (M. Armstrong), hamid.mehrabi@sunderland.ac.uk (H. Mehrabi), nida.naveed@sunderland.ac.uk (N. Naveed).

https://doi.org/10.1016/j.jmapro.2022.10.060
Received 17 July 2022; Received in revised form 24 September 2022; Accepted 17 October 2022

Nomenclature

3D	three-dimensional
ADAM	atomic diffusion additive manufacturing
AM	additive manufacturing
ANN	artificial neural network
ASTM	American society for testing and materials
BJ	binder jetting
BMD	bound metal deposition
BSL	binder saturation level
CAD	computer-aided design
CAM	computer-aided manufacturing
CNC	computer numerically controlled
DED	directed energy deposition
DfAM	design for additive manufacturing
DM	desktop metal
EBM	electron beam melting
EE	energy efficiency
FDM	fused deposition modeling
FM	formative manufacturing
GE	General Electric
HAM	hybrid additive manufacturing
HAZ	heat-affected zone
HIP	hot isostatic pressing
ISO	international standards organisation
LBM	laser beam melting
LCA	life cycle assessment
LMD	laser metal deposition
LoF	lack of fusion
LT	layer thickness
MAM	metal additive manufacturing
ME	material extrusion
MIM	metal injection molding
mf	manufactures standard
ML	machine learning
mLS	metal laser sintering
NNS	near net-shaped
PBF	powder bed fusion
PM	powder metallurgy
RS	residual stress
SLM	selective laser melting
SLS	selective laser sintering
SM	subtractive manufacturing
SS	stainless steel
STL	standard tessellation language
Sy	ultimate tensile strength
Su	yield strength
TM	traditional manufacturing
TS	tool steel
WAAM	wire arc additive manufacturing

composites [6]. Among them, arguably, metal AM (MAM) has shown the most significant impact across various industries. For instance, in the medical sector, MAM has been successfully used to print a number of surgical titanium implants recently [7]. In the aviation industry, the 300 parts used to make up the heat exchanger assembly in the GE9X engine for the Boeing 777× have been reduced to a single component that is 40 % lighter and 25 % cheaper [8]. SpaceX also reduced the production time for its Super Draco engine as well as the weight of their Raptor engine by 40 % [8,9], and NASA will soon replace the main engine for the Space Shuttle with MAM parts in order to also reduce production time and weight [9]. In the construction industry, MAM was recently used to manufacture the world's first printed metal bridge from 308LSi austenitic stainless steel (SS), which spans 10.5 m over the Oudezijds Achterburgwal canal in De Wallen, Amsterdam [10]. As a result of case studies such as these and reports of rapid growth rates [11], the profile of additive technologies has increased dramatically, resulting in a greater emphasis on their ability to produce reliable and reproducible mechanical properties.

Consequently, various communal limitations have been identified regarding different failure modalities, such as low plasticity and reduced fatigue performance, among others [12]. Some of these have been attributed to microstructural discontinuities arising from defects such as high residual stress (RS), surface roughness, lack of fusion (LoF), high porosity, shrinkage, and distortion [13]. There is also evidence that the mechanisms underlying these defects are associated with the complex thermal actions metal parts undergo during printing, such as rapid heating, cooling, and solidification, leading to microstructures and mechanical properties that differ from those produced traditionally [14]. Equally, it has also been recognized that the process parameters can significantly influence the prevalence of these defects, some of which include layer thickness (LT), build orientation, input power, span speed, hatch spacing, infill, and scan strategy, among others [15–20]. It is important to note, however, that, unlike established metalworking techniques which have produced consistent properties over an extended period of time, a similar understanding of the relationship between processing, structure, and property for MAM is still underdeveloped, which is one of the most pressing research issues in additive technology. [21–23]. Despite these specific challenges, certain scenarios exist where MAM is well suited for various applications, with clear technical advantages over TM processes. For instance, the cost of casting or machining a product is directly proportional to its complexity [24]. Features with sharp internal corners, cavities, or thin walls may require more process operations, and different tooling, resulting in increased production time. Similarly, complexity increases when tight tolerances or good surface finishes are needed. Comparatively, adding material layer by layer to create a 3D part means that MAM is not limited by the same limitations, which is why it is often described as a process where complexity is free. [25]. Nevertheless, some have argued that as complexity increases, print times and the quantity of material required may also increase [26]. Rather, it has been suggested that complexity is preferred would be more appropriate [27]. This means that MAM is most beneficial with components that have either complex geometric features or internal lattice-type structures, similar to natural materials such as the porous interior of a bone. In this way, the part's mass can be significantly reduced by only assigning material where it is structurally necessary, thereby reducing the amount of material required, reducing print times, and improving the EE of the printing process. It is also known that certain alloys can be difficult to process with traditional methods [28]. For instance, most nickel-based superalloys are notoriously difficult to machine as they are liable to resist shear, tension, and compressive forces. The high nickel content tends to lead to workpiece hardening, which significantly increases the cutting pressure leading to deformation and eventual tool wear [29]. MAM is able to print many of these hard-to-process materials without expensive tooling, especially for intricate parts with internal fluid channels, such as heat exchangers [30]. In addition to geometric benefits, MAM has been shown to reduce production time by eliminating process steps inherent to TM techniques [31]. When working with MAM, powders, wire, and other feedstocks are typically purchased off-the-shelf and can be instantly loaded into the printer. This is in contrast to the foundry workflow, where raw material must be melted, refined, and held before pouring the molten metal. By printing components near net shaped (NNS), which refers to parts that are geometrically as close to the final design as possible, the need for designing, analyzing, and fabricating tooling, jigs, patterns, and molds

can also be eliminated, along with the byproducts of CNC machining such as metal chips. In most cases, however, printed parts require some form of post-processing, such as machining, in order to remove build plates and support structures and to improve tolerances [32]. Other processes may also be needed, such as thermal debinding and sintering, in order to dissolve residual filament and achieve densification. For tailoring the mechanical properties of printed parts, it may also be necessary to perform post-heat treatments, such as hot isostatic pressing (HIP), aging, or annealing [33]. A wide range of materials have been developed specifically for MAM. These include aluminum alloys, stainless steel, nickel-based superalloys, titanium alloys, cobalt alloys, and refractory alloys, among others [22]; and their commercial availability, as well as their mechanical properties, are outlined throughout this article. Powder-based materials are most commonly used, although wire is also used in some cases; both materials are processed by melting or sintering, followed by solidification using energy sources such as lasers, electron beams, or heated nozzles [8]. In general, MAM processes are categorized according to ASTM/ISO 52900:2017 [5] into seven broad categories: material extrusion (ME), binder jetting (BJ), powder bed fusion (PBF), directed energy deposition (DED), sheet lamination, and vat polymerization. Among these seven processes, only four relate to metals.

As one of the most commonly used processes, PBF is increasingly being used to manufacture products in industries including aerospace, medical, automotive, industrial, tooling, and consumer goods [34]. With these technologies, a fine layer of powder is deposited over a build plate, and an energy source is used to selectively melt or sinter a cross-section of the part into the powder layer. It is possible to further define PBF technologies based on their melting mechanism. In the case of laser-based machines, they typically fall into either selective laser melting (SLM) or selective laser sintering (SLS), whereas those utilizing electron beams are referred to as electron beam melting (EBM). As a popular process for repairing and adding material to existing parts, DED can be used with either wire or powder as the feedstock. [35]. As with PBF, lasers are typically used in DED to fuse the material; however, the main difference is that both feedstock and the energy source are usually located on the same print head. Powder-based DED machines are sometimes referred to as laser metal deposition (LMD) machines, while wire-based machines are known as electron beam-AM (EBAM) and wire arc-AM (WAAM). A variety of technologies also exist for BJ, such as nanoparticle jetting (NPJ), single-pass jetting (SPJ), and supersonic deposition (SD). BJ creates parts using a print head similar to a 2D printer that deposits liquid binder droplets layer by layer. When compared with PBF and DED, BJ offers two significant advantages. Firstly, multiple heads can be used simultaneously to print at several locations, allowing machines to print much faster [36]. Secondly, the machine is capable of producing low to medium numbers of identical parts, and batch production processes can be managed with the help of a large furnace for sintered parts [37].

Contrary to most other processes and as one of the most cost-effective methods for printing metal parts [38], ME does not involve the use of loose powder or wire. The particles of metal powder are instead bound together in a polymer filament similar to the feedstock used in metal injection molding (MIM). As with fused filament fabrication (FFF), ME feedstock is extruded through a heated nozzle onto a build plate to construct the part incrementally. Aside from printing, ME requires two post-processing steps: first, a debinding stage to dissolve the polymer binder, and second, a sintering step. Each of the technologies described above has its roots in TM processes, regardless of whether it's powder metallurgy, welding, or another type of metalworking technique. In spite of the extensive knowledge base that exists for some of these conventional processes, it does not reflect the unusual characteristics that printed parts exhibit, nor does it address many of the current technical challenges for additive methods, despite its advantages and recent developments. Based on the decades of research efforts that have resulted in a fairly mature knowledge base for these established techniques, it would seem that our understanding of printing metals could also follow a similar timeline.

Research efforts have increased significantly to accelerate the development of MAM recently. However, most publications are dispersed over a variety of journals, reports, and various other sources. Because of this and other factors, there is a significant lack of experience in the industry. Technologists may have some knowledge of one or more of these topics; however, few individuals possess a comprehensive understanding of all of these subjects. As a result, companies have limited access to expertise in order to take advantage of the benefits of MAM. In order for MAM to be widely adopted, it will be necessary to overcome the limited foundational understanding of additive technologies that currently exist within the workforce. In order to fully appreciate the advantages and disadvantages of MAM to decision-makers, technical experts need to have a thorough understanding of its capabilities and limitations. Therefore, a single reference source featuring evidence that is both up-to-date and empirical would be useful in supporting academia as well as industry in filling this gap. In light of this, periodic reviews of current research understandings and needs are essential. While there are many excellent and detailed review papers on MAM, which are briefly discussed below, it is important to keep in mind that this industry is rapidly growing and that new technologies and discoveries are often being made. As a result, it is common for review papers that are several years old to be outdated. There are also some that focus solely on specific themes, such as defects, processing parameters, optimization methods, and mechanical properties. In view of these factors, it is often challenging to evaluate the benefits and limitations of MAM compared with traditional methods. Therefore, this review article provides an overview of the process characteristics of the most commonly used MAM technologies today and a summary of their mechanical properties alongside reference values for a number of TM methods. An evaluation of the current knowledge base of each MAM classification is performed as part of this review in order to determine what opportunities exist for future research. Thus, the scientific contribution and novelty of the present work is an in-depth review of the current state of the technology, the gaps in the literature, and the research needs that will benefit the expansion and advancement of MAM in the future. In the same vein, the present work differs from other review articles as it also provides a distinct perspective on the sustainability credentials of MAM when compared to TM. This is done by providing extensive evidence of the most recent research in this area, including the specific energy consumption (SEC) required to print 1 kg of material for a variety of MAM technologies and a framework to improve the EE of printing metallic components. Due to its comprehensive examination of both the process characteristics and the environmental impact of MAM, the current paper offers an in-depth understanding of it from a holistic perspective, which is especially valuable for researchers and technologists approaching the subject for the first time.

2. Review structure, objectives, and limitations

This review draws on a variety of sources, including peer-reviewed journal articles and international standards. Furthermore, industrial publications from commercial data are used when there is no information in the scientific literature (e.g., mechanical data). Although this review article cites unsubstantiated data, it recognizes the need for further research. As a result, this article provides a concise overview of MAM technology. It can serve as a starting point for identifying potential research topics to study in the future, especially if comparisons are to be made with materials manufactured using TM processes. These materials are marked as manufactures (*mf*) standard. While there are a large number of publications on MAM, there are only a few review articles that summarize the technologies, challenges, and applications related to this field. The purpose of this section is to provide a brief overview of the major findings of these previous articles. It also aims to evaluate whether any significant changes have been made since publication. A generic

MAM workflow is then presented, followed by a more detailed analysis of the literature regarding each MAM process. Finally, a segment is devoted to sustainability by summarizing the latest research findings.

Before ASTM/ISO 52900:2017 [5] was developed, Frazier [39] evaluated MAM and used the terms powder bed, powder feed, and wire feed to distinguish the technologies. An analysis of the microstructural properties of several materials was also performed, with Ti-6Al-4 V being the focus, followed by a review of the mechanical properties of other various materials. It is important to note that at the time of this review, materials were limited in availability, especially for commercial use. There is a discussion of the challenges associated with MAM's certification, followed by a consideration of the business case and environmental implications of MAM technology. The main findings of this review paper were that material anisotropy, the lack of established standards for the qualification of parts, the high cost of feedstock, and an inadequate understanding of the environmental implications all served as fundamental barriers to the adoption of MAM at that time. An in-depth review of the processing defects, thermal histories, post-processing, microstructure, and mechanical properties related to directed DED and PBF was provided by Sames et al. [40], with a particular focus on comparing the limitations of these two technologies. The review notes that some applications do not require parts to undergo post-processing since the as-printed microstructure is sufficient. However, many applications do require post-processing. As a result, the review highlights the importance of characterizing as-printed microstructures in order to develop printing processes that entail little or no post-processing in the future. Furthermore, the study discusses future research topics based on the limitations of the technology. These include faster deposition rates, improved quality control, the reduction of human input through more reliable machines, a reduction in hardware and feedstock costs, and the development of a broader range of materials. Laser beam melting (LBM), EBM, and LMD were considered the most popular MAM technologies at the time Herzog et al. [33] published their review. This article mainly focuses on the relationship between process parameters, microstructure evolution, and mechanical properties. A helpful description concerning feedstock production is also provided, along with an explanation of how powder production can affect certain characteristics, such as particle morphology, particle size, and chemical composition. Finally, the microstructure and mechanical properties of various metals are considered. The authors acknowledge at the time of this review that attempts to fully characterize anisotropy would be a significant advancement in the field of MAM.

Zhang et al. [41] reviewed the latest developments and the process characteristics of PBF, DED, BJ, and sheet lamination. Additionally, the microstructural and mechanical properties of each process were compared and evaluated. Furthermore, data on the properties of various commercial systems were collected and compared with those of wrought metals. The results of this study indicated that the correlation between process parameters and material properties, and microstructure has not yet been fully understood. In order to understand the relationship between structure and property, the authors suggested that a number of theoretical models, such as heat and mass transfer, residual stress, and distortion evolution, are explored. For improved production efficiency, they also propose optimizing the process parameters in the future for both the design and the implementation of MAM methods, such as efficient heat treatment. As a final step, materials databases, as well as technical standards, should be developed in order to avoid repeatability issues.

The mechanical properties of metal parts manufactured by PBF and DED have recently been examined by Haghdadi et al. [21]. As part of this review, austenitic, maraging, and precipitation hardened (PH) steels were discussed in depth, as well as notes regarding the influence of various post-processing heat treatments on the microstructure, mechanical properties, and corrosion properties of these metals within each classification. Moreover, a valuable section discusses some common challenges associated with MAM, including residual stresses, anisotropy, and porosity. At the time of publication, 17–4 precipitation-hardened (PH) SS was the most popular material, and PBF and DED were the most common printing machines. Additionally, the researchers noted that MAM could enhance pitting corrosion resistance in austenitic steels because manganese sulfide inclusions (MnS) cannot form during rapid solidification, and some defects may not be remedied by post-processing heat treatments. As a result, it may be necessary to develop more effective heat treatments. Finally, as a result of the complex thermal cycles that printed parts undergo, unique microstructures can be produced, which differ from those produced by subtractive manufacturing (SM) and formative manufacturing (FM) processes. While these findings are encouraging, this particular review is primarily focused on material characteristics, not providing a comprehensive overview of MAM's general challenges and issues.

The most noteworthy feature of the above reviews is that none compares MAM with TM and only Frazier discusses the lack of research that has been conducted to evaluate the sustainability of MAM. Several studies are cited by Frazier to assess their idea based on energy efficiency (EE) and suggest that it should be compared with TM. Additionally, no discussion of ME technology is included in any of these articles. Nevertheless, it is important to keep in mind that some progress has been made since these reviews were published. Because this field is undergoing rapid development, a contemporary perspective would be helpful. Moreover, the subject of MAM is comprehensive, which limits the amount of information that can be conveyed in a single article. The present review is organized into eight parts. Section 3 describes a typical MAM workflow. Each MAM category and its corresponding technologies are described in Section 4. ME is characterized in Section 5, BJ is characterized in Section 6, PBF is characterized in Section 7, and DED is characterized in Section 8. A summary of current knowledge regarding sustainability issues is presented in Section 9. In Section 10, the entire subject is recapitulated, and the main challenges for each technology, including the matter of sustainability, are summarized individually.

3. The typical MAM workflow

Fabricating a metal structure with MAM involves several stages. The manufacturing workflow for one product may differ from those for another depending on the product being created. Similarly, depending on the application, a prototype part may only require printing in order to determine its suitability before committing to the production of large quantities. On the other hand, parts that are intended to replace high-value, structurally significant components may require various post-processing treatments and quality inspections prior to their use. In general, however, these processes can all be summarized in one flow diagram, as illustrated in Fig. 1. These stages are briefly described one by one in the following paragraphs.

3.1. Design

The origin of all additive parts is a digital representation of the physical product. This can be achieved with a 3D CAD model incorporating all geometric features as well as additional ones, such as internal infills and support structures.

3.2. Conversion

After the design has been completed, the issue of interoperability must be addressed, which refers to the ability of digital technologies to exchange and make use of information with each other. For this reason, a file must be translated into data that can be understood by the MAM machine. This is achieved by converting the 3D CAD file into a standard tessellation language (STL) file.

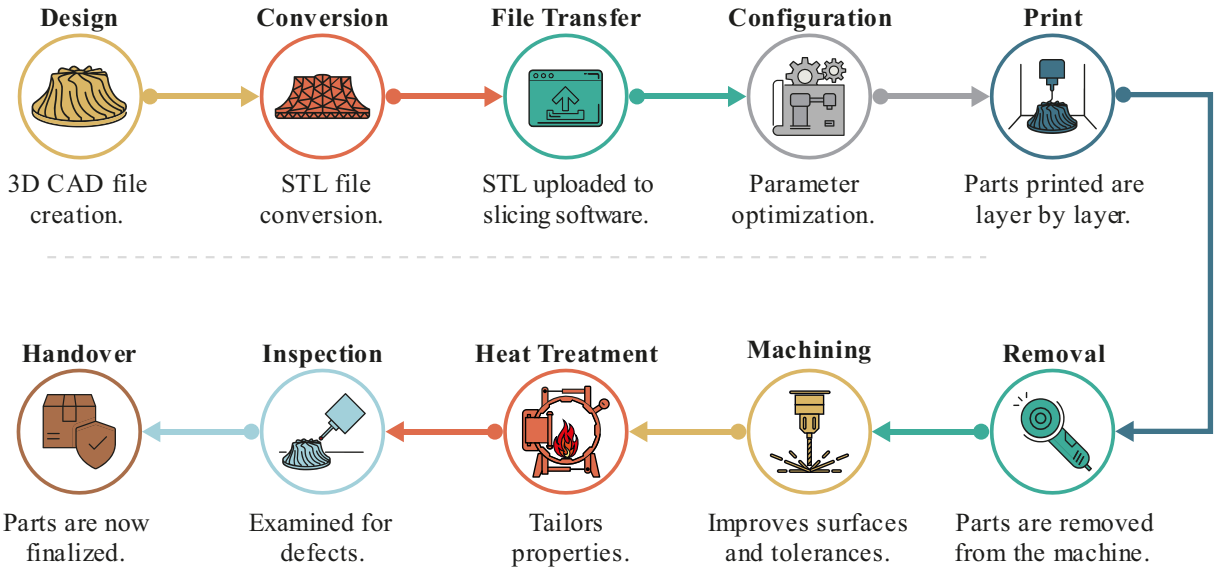

Fig. 1. An example of a typical MAM process workflow.

3.3. File transfer

The STL file can then be transferred to the MAM machine or uploaded to a 'slicer' software such as Markforged Eiger platform, which converts the 3D data into 2D layers or slices, which can be used to calculate the tool path or G-Code needed to manufacture the object.

3.4. Configuration

Prior to printing, the MAM machine must be properly configured and variables set. Settings of this type would include those related to the process parameters, such as the orientation of the parts, the thickness of the layer, and the inclusion of rafts, among others. The slicing software can also be used to adjust and select these parameters.

3.5. Print

The printing phase can vary greatly depending on the technology employed. Depending on the geometry and size, printing is typically the most time-consuming activity taking anywhere from a few hours to several days to complete. However, the printing process is the one activity that requires very little human intervention apart from intermittent monitoring of the progress.

3.6. Removal

Once parts are fabricated, they can be removed from the build chamber. Process dependant, parts can also be subjected to a debinding stage to dissolve excess material or sintered in a furnace to achieve part densification.

3.7. Machining (optional)

Depending on the intended application, post-processing machining can be carried out to improve tolerances or surface finishes. Build plates and any other auxiliary features, such as support structures, can also be removed either physically or mechanically with either wire EDM or band saws.

3.8. Heat treatment (optional)

The complex thermal cycles that metal parts are subjected to can often cause a buildup of internal stresses, and heat-treating parts can relieve this. Furthermore, different types of heat-treating methods can be used to tailor the mechanical properties and reduce porosity. These can include HIP, annealing, and aging, among others.

3.9. Inspection (optional)

Finished parts can also be subjected to external non-destructive tests (NDT) such as fluorescent liquid penetrant (PT), visual (VT), surface roughness, and dimensional accuracy. Internal radiography (RT), electromagnetic (ET), and ultrasonic (UT) to check for defects.

3.10. Handover (optional)

After quality assurance, parts are ready to be used and handed over to the customer.

4. MAM classifications and commercial systems

Table 1 lists the four MAM categories defined by ASTM/ISO 52900:2017. Table 2 lists the commercial availability of various commercial ME systems along with Table 3 for BJ, Table 4 for PBF, and Table 5 for DED. The following sections in this article will consider a selection of these machines from each category and report on their mechanical properties. These are then compared against values for some

Table 1
MAM processes modes and applications [5].

Process	Abbreviation	Mode	Typical Applications
Material extrusion	ME	Material is selectively dispensed through a nozzle or orifice	Functional metal parts, prototyping,
Binder jetting	BJ	A liquid bonding agent is selectively deposited to join powder materials	Functional metal parts, low-rate production runs of non-critical components
Directed energy deposition	DED	Focused thermal energy is used to fuse materials by melting as they are being deposited	Functional metal parts, repairs, adding material to existing parts
Powder bed fusion	PBF	Thermal energy selectively fuses regions of a powder bed	Functional metal parts, functional prototyping

Table 2
Commercial ME machines.

Process	Technology	Manufacturer/ Machine	Build volume, mm	Country	Ref.
ME	Atomic diffusion additive manufacturing (ADAM)	MarkForged Metal X	300 × 220 × 180	US	[42,43]
	Automated multi-material deposition (AMD)	TRIDITIVE AMCELL	Ø220 × 330	ES	[43]
	Bound metal deposition (BMD)	Desktop Metal (DM) Studio System	289 × 189 × 195	US	[43,44]
	Pellet additive manufacturing (PAM)	Pollen AM PAM Series M	Ø300 × 300	FR	[43]

Table 3
Commercial BJ machines.

Process	Technology	Manufacturer/ Machine	Build volume, mm	Country	Ref.
BJ	BJ	ExOne X1	800 × 500 × 400	DE	[37]
	BJ	ExOne Innovent+	160 × 65 × 65	DE	[45]
	BJ	DM Shop System	350 × 220 × 50–200	US	[46]
	Single pass jetting (SPJ)	DM Production System	490 × 380 × 260	US	[47]
	Supersonic deposition (SD)	SPEED3D LightSPEE3D	300 × 300 × 300	AT	[48]

Table 4
Commercial PBF machines.

Process	Technology	Manufacturer/ Machine	Build volume, mm	Country	Ref.
PBF	DMLM	GE Additive M2 Series 5	250 × 250 × 350	US	[49]
	DMLS	EOS M 100	Ø100 × 95	DE	[50,51]
	DMLS	EOS M290	250 × 250 × 325	DE	[50,51]
	SLM	Coherent Creator	Ø100 × 1000	DE	[51]
	SLM	RenAM 500	250 × 250 × 350	UK	[51]

Table 5
Commercial DED machines.

Process	Technology	Manufacturer/ Machine	Build volume, mm	Country	Ref.
DED	LMD	Meltio M450	150 × 170 × 425	DE	[52]
	DED	DMD 500D	1219 × 1219 × 600	US	[53]
	Laser-engineered net shaping (LENS)	Optomec CS 1500	900 × 1500 × 900	US	[54]
	DED	DMG Mori Lasertech 65 DED	735 × 650 × 560	UK	[54]

TM methods.

\

5. ME technology

The ME market accounted for 10 % of all MAM sales in 2020 [55] and, compared to other technologies, is said to be more EE as there is no demand for high-energy lasers. It is also easier to operate [56] and 60–80 % more economical than PBF [44]. First patented in 1988 by S. Scott Crump of Stratasy Inc., it was named fused deposition modeling (FDM) and was primarily used for layer-wise polymeric and composite manufacturing [57]. The patent expiration in 2009 paved the way for several manufacturers to develop proprietary technologies founded on FDM. Consequently, various systems based upon the initial patent have emerged since then. Despite this, only commercially available metal ME systems in Table 2 are reviewed in this work.

5.1. ME process

ME is characterized by the extrusion of the material to create a 3D part. Unlike other MAM processes that utilize loose metal powder, ME machines consume a flexible feedstock similar to MIM media composed of metallic powders bound in a polymer matrix that functions as the binding system giving rise to a safer feedstock [38]. A typical ME machine represented in Fig. 2 (a) will extrude the bound powder in addition to ceramic release material stored on a separate spool in a heated chamber. The feedstock is heated to a temperature above the polymer binders' melting point via the heated print head (Fig. 2 (b)), extruding the softened material onto a heated build plate. The build plate travels on the vertical z-axis, extruding material in separate layers equidistant to the preceding layer; simultaneously, the print head attached to a gantry system moves in the perpendicular (x, y) plane to form the shape of the part.

At the same time, ceramic release material is deposited between the part and any overhanging support structures and the build plate, allowing ease of separation after printing. Extruding material layer upon layer tends to give rise to anisotropy that can be caused by the introduction of voids (Fig. 3 (a)) or ‘air gaps’ between each deposit that can compromise the adhesion between each layer [15,58]. Consequently, the strength of the bond and, to a greater extent, the metal part is the weakest perpendicular to the plane of material deposition [59]. ME also produces parts with mediocre surface finishes due to the nozzle's circular profile, where the bound powder is compressed and deformed into a quasi-elliptical shape against the previous layer, illustrated in Fig. 3 (b). Thus, ME parts inherently include undulating side profiles and notches between layers which cause undesirable stress concentrations. Hence, post-processing machining is advised.

Next, the as printed or ‘green’ part is debound through a ‘washing’ process. The fragile and lightly bound workpiece represented in Fig. 4 (a) is placed inside a heated debinding machine, initially dissolving a proportion of the binder system's core component in a solvent illustrated in Fig. 4 (b). The binder systems can influence the production process and quality of the finished component and has a typical constitution of three parts: polymers, waxes, and additives and can be further defined as the core, the backbone, and the additive [38]. The core component accounts for 50–90 % of volume, where materials used are those with low viscosity, are dissolvable, and can undergo catalytic degradation (e.g., elastomers, waxes, and amorphous polyolefin), which are easily removed in the initial debinding stage. The backbone component accounts for 0–50 % of the volume, where materials used tend to be resistant to debinding solvents, which helps retain the strength of the debound part before sintering, such as polyolefins. The final additive can account for 0–10 % volume of the binder system. It can be composed of plasticizers, tackifiers, and compatibilizers, among others, that can help to increase the adhesion of each successive layer or add flexibility to the otherwise rigid filament to store in a spool [38,60]. The core component

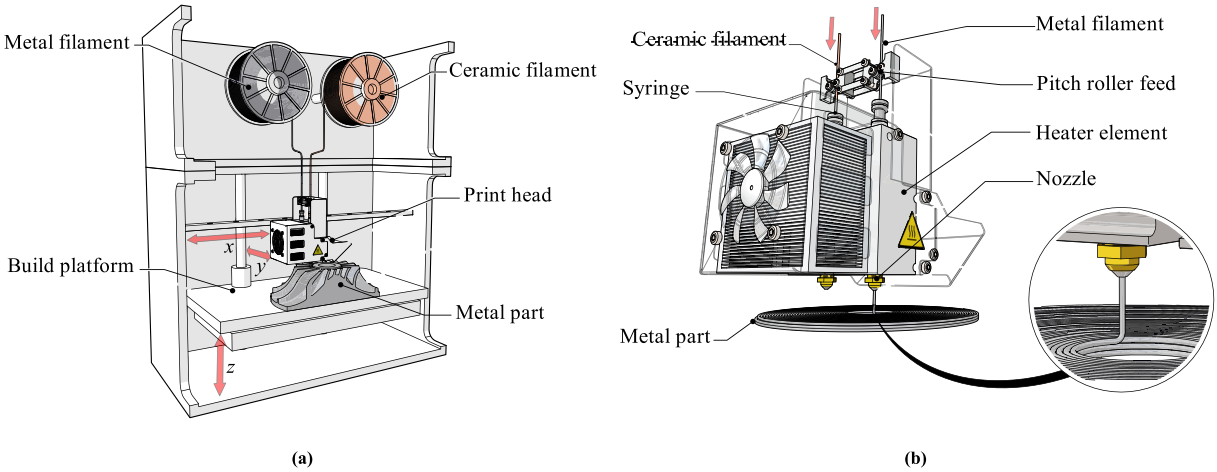

Fig. 2. (a) Schematic of a ME machine (b) Schematic of a typical ME print head mechanism.

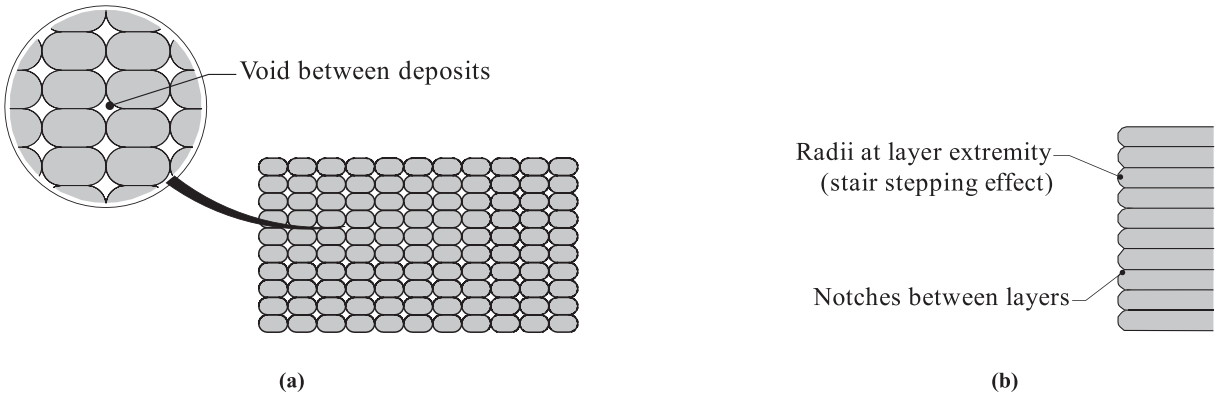

Fig. 3. (a) Schematic of voids between extruded deposits (b) Schematic of radius and notches in extrude material layers.

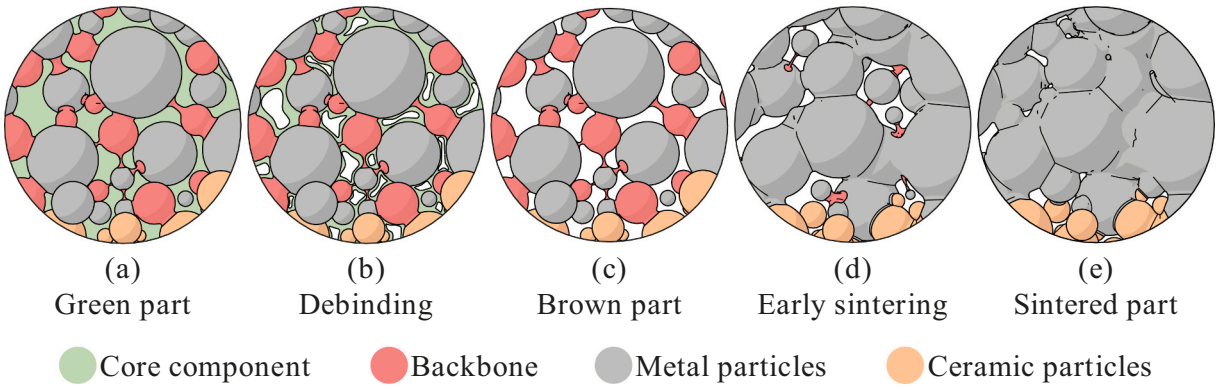

Fig. 4. Schematic of feedstock morphology - adapted from [38] (a) as printed, (b) debinding - thermal decomposition of the core binder component, (c) brown part – following the debinding process, (d) early-stage sintering – thermal decomposition of the residual backbone (e) sintered – thermal densification of metal powder particles. (For interpretation of the references to colour in this figure legend, the reader is referred to the web version of this article.)

is eventually dissolved, leaving only the backbone in place, and is referred to as being in its 'brown' state, retaining much of the backbone; nonetheless, it is still highly porous (Fig. 4 (c)). The part is then placed inside a furnace and is gradually heated from an ambient temperature to 70–90 % of the metal's melting point [38], thermally decomposing the residual support component of the binder system shown in Fig. 4 (d). As temperatures rise inside the furnace, solid bonds or necks form between the metal powder particles, reducing the surface energy of the part [61]. As temperatures reach the metal's melting point, atomic diffusion of metal particles occurs, leading to the formation of solid bonds, reducing porosity, and transforming a lightly bound metal powder into a 96–99.8 % theoretically dense metal part [44,62,63] (Fig. 4 (e)). This densification results in shrinkage of the part by 12–20 %, which the systems software accounts for during the file transfer stage.

5.2. *Material characterization of ME*

Despite modest commercial availability of materials for ME

Table 6
Commercial material availability for ME [43].

Metal categories	Alloy	ADAM	BMD
Stainless steel	17–4 PH SS	×	×
	316 L SS	..	×
Tool steel	H13	×	×
	A2	×	..
	D2	×	..
	4140	..	×
Nickel alloy	IN625	×	..
Copper	Copper	×	×

(Table 6), it is reported that other materials, such as titanium alloys and aluminum alloys, are in development [62]. Data for commercially available materials are shown in Tables 7, 8, and 9. Results are compared for both the Metal X (ADAM) and DM Studio System (BMD) for 17–4 PH SS, H13 tools steel (TS), and copper, where wrought and MIM material equivalents are included for comparison. Typical material properties appear promising, with the Metal X and Studio System usually outperforming MIM in the as-sintered state except for BMD copper elongation.

5.3. Process characteristics of ME

A broad body of knowledge exists for mature extrusion-based processes such as FDM and FFF, and a comprehensive explanation can be found in [38,69]. Conversely, only a limited amount of research has been conducted to characterize modern ME processes. Since newer technology is based on these mature extrusion techniques, it is helpful to discuss previous reports to understand the similarities. One of the most common causes of defects in mature extrusion-based processes is anisotropy [17]. This is said to be caused by the linear formation of intra-filament pores at the interface between solidified layers caused by the spherical profile of the extrusion nozzle [15,58]. These pores produce localized stress concentrations that compromise the strength of bonds and can result in structures prone to premature failure in the plane parallel to the direction of a load and that build orientation, and LT can significantly influence their manifestation [59]. For example, studies have shown that FFF tensile samples printed perpendicular to the loading direction (flat and on-edge) demonstrate the highest strength, whereas samples printed parallel to the loading direction (vertical) exhibit the lowest strength [16]. Other studies have also confirmed that flat and on-edge samples outperform vertically printed samples and have a higher relative density [20,70–72]. It has also been shown that minimal LT can similarly improve tensile in addition to reducing pore size, thereby improving overall density [16]. However, other studies have reported the opposite effect [73]. For instance, increasing the LT has improved the tensile strength of some parts. It is believed this could be the result of reducing the number of filament strands and, therefore, interfaces between bonds, which, in turn, could result in fewer intra-filament pores. However, another similar study revealed conflicting findings when the density of printed parts was found to be negligible after altering the LT [74]. In terms of work done for modern ME technologies, it has been shown that BMD parts can exhibit similar mechanical properties to MIM by orienting parts flat and with rafts [44]. For example, sintered samples were shown to have a tensile strength of 776 MPa in one study, which is in the range for MIM, at 775 to 950 MPa. However, stiffness in these parts can be reduced by as much as 7 %, although it is believed that this can be negated by improving surface finishes through machining. However, this has not been demonstrated. Thus, it would be helpful if future work was carried out to determine the influence of post-processing on BMD parts. There has also been a recent attempt to manufacture a Sterling engine from 17 to 4 PH SS to understand the challenges associated with designing and manufacturing metal parts using BMD [75]. One of the main issues was the significant deviations observed up to 0.50 mm in some areas with high aspect ratios compared with the original 3D CAD model. Though, it might be possible to compensate for this by adjusting the thicknesses of features during the design stage. Nevertheless, this example shows that care should be taken when designing products where critical elements have high aspect ratios or are relatively thin. Like BMD, only a narrow scope of literature exists for the ADAM process. Among some of the work done, it has recently been shown that the density of sintered parts with solid infill was comparatively low (90 %) [42]. It is interesting to note that these observations conflict with data that has been published by the Markforged and others who claim that 99.7 % is achievable [62]. The LT for the ADAM process can also influence the microstructural characteristics of printed parts [56]. An analysis of samples printed in various orientations shows that parts exhibit increased strength along planes parallel to the extrusion direction and weakest orthogonal to the extrusion direction [20]. Overall, research has shown similarities in the characteristics of parts printed with modern and mature ME processes. Although it has been comprehensively demonstrated that vertically printed parts exhibit weaker tensile properties compared to other orientations, there is insufficient evidence that establishes similar relationships between printing metallic parts, either flat or on-edge, particularly for the ADAM process. Furthermore, the effect of LT has not been adequately investigated, and studies contradict one another regarding its impact on mechanical properties. In order to achieve high-quality metal parts by ME, it is crucial to understand and report on these influential variables. Consequently, further studies must be conducted to characterize the microstructure and mechanical properties of metal components manufactured in this manner. To better appreciate the differences between various manufacturing techniques, these properties should also be compared with parts manufactured using TM processes such as casting, turning, and milling, for example. It is also noteworthy that several of these studies highlight the disparity between manufacturers' data; therefore, this is another area worthy of investigation. A summary of the advantages and disadvantages of ME is described in Table 10.

6. BJ technology

Metal BJ can trace its origins back to 1993 when the technology was developed by MIT's Sachs et al. [57] and later patented as ‘three-dimensional printing’ (3DP), a universally accepted term for most AM technologies. The ExOne Company attained sole licensing of MIT's patent in 1996, yet it was revised in 2004, allowing Z Corporation exclusivity to its use. Since then, and with the patent's expiration, many companies have developed various metal BJ technologies, with several of these presented in Table 4. Unlike other MAM machines that consume

Table 7
Comparison of reported mechanical properties of 17–4 PH SS for ME.

Alloy	Process	Reported by	Machine	Orientation	Condition	UTS, MPa	YS, MPa	El, %	Ref.
17–4 PH SS	Wrought	CES Granta	…	…	H900 Heat-treated	1379	1233.5	15	[64]
	Cast	CES Granta	…	…	H900 Heat-treated	1306.5	1161	4.35	[64]
	MIM	Watson et al.	…	…	As sintered	775–950	675–775	5–7	[44]
	ME	(*mf*) Markforged	Metal X (ADAM)	Horizontal	As sintered	1050	800	5	[20]
	ME	Henry et al.	ADAM	All	As sintered	776–999	580–765	0.76–3.2	[20]
	ME	(*mf*) DM	Studio System (BMD)	Horizontal	As sintered	1042	660	8.5	[44]
	ME	Watson et al.	BMD	All	As sintered	776	604	6.7	[44]

Table 8
Comparison of reported mechanical properties of H13 tool steel for ME.

Alloy	Process	Reported by	Machine	Orientation	Condition	UTS, MPa	YS, MPa	El, %	Ref.
H13	Wrought	ASM	…	…	Heat-treated	1580	1360	14	[65]
	Hot work	CES Granta	…	…	Annealed	1990	1650	9	[64]
	ME	(*mf*) Markforged	ADAM	Horizontal	As sintered	1420	800	5	[65]
	ME	(*mf*) Markforged	ADAM	Horizontal	Heat-treated	1500	1250	5	[65]
	ME	(*mf*) DM	BMD	Horizontal	As sintered	1325	650	2.3	[66]
	ME	(*mf*) DM	BMD	Horizontal	Heat-treated	1720	1250	5.8	[66]

Table 9
Comparison of reported mechanical properties of copper for ME.

Alloy	Process	Reported by	Machine	Orientation	Condition	UTS, MPa	YS, MPa	El, %	Ref.
Copper	Cast	CES Granta	…	…	H.C. copper	152.5	34	23	[64]
	MIM	MPIF Standard 35	…	…	Heat-treated	207	69	30	[67]
	ME	(*mf*) Markforged	ADAM	Horizontal	As sintered	193	26	45	[67]
	ME	(*mf*) DM	BMD	Horizontal	As sintered	195	45	37	[68]

Table 10
Summary of the advantages and disadvantages of ME.

Advantages	Ref.	Disadvantages	Ref.
Relatively safer feedstock.	[38]	High porosity.	[42]
Relatively economical.	[44]	Poor surface finishes because of the stair-stepping effect.	[15,38,58]
Easy to use.	[38]	Typically requires a debinding stage to remove polymer binder.	[38]
Relatively high geometrical accuracy.	[56]	Anisotropy typical due to voids between layers.	[15,38,58]
		Strength is reduced in the plane perpendicular to the extrusion direction (z-direction).	[59]
		Requires support structures for overhanging and unsupported features.	[38]

comparatively large amounts of energy, BJ machines (Fig. 5) require significantly fewer resources as no lasers, or electron beams are needed. Although many variations of the original design have emerged since 1993, ExOne and DM machines are reviewed, and mechanical properties are compared. There have been several comprehensive reviews on the BJ process [41,76]; however, the following section provides a brief overview.

6.1. BJ process

Like printing ink onto paper, BJ performs similarly. Rather than printing in two dimensions (x, y), the process exploits the third dimension (z) to create a solid part when metallic powder particles adhere to one another via a liquid binder. Printing typically occurs at ambient temperature [77], which helps to eliminate thermally induced defects such as undesirable grain growth and distortion inherent with other heat source-reliant MAM processes [78]. In addition, the surrounding metal powder functions as a temporary surrogate support structure. Thus, minimal waste is produced as no support structures are needed [76]. At the outset, a fine layer of loose metallic powder fed from a powder hopper is deposited onto a build platform via a re-coater, resulting in a typical LT of 50–200 μm. Then, via the inkjet printhead illustrated in Fig. 5 (b), moving in the x- and y-direction, droplets of liquid binder are selectively deposited onto the existing powder shown in Fig. 6 (a). The effect of capillary pressure, and to a lesser extent, gravitational forces, coerce each droplet of binder to infiltrate and flow into the voids between the metal powder particles (Fig. 6 (c)) to achieve a uniform distribution (Fig. 6 (d)) [79].

This binder distribution versus powder, known as the binder saturation level (BSL), determines the green parts' mechanical strength, surface finish, and tolerance [80], where the BSL parameter is dependent on the capacity of the inkjet print head [81]. A heated or ultraviolet lamp then passes over the initial layer to dry and cure the binder; this sequence is represented in Fig. 6. Following the binding and curing of the initial layer, the build plate moves in the negative y-direction equidistant to the first layer, where the re-coater applies the next layer of loose metal powder, and the additional binder is deposited. Replication of this process follows until the part is finalized. Although bound, the part is fragile, surrounded by excess metal powder, and has a relative composition of 25–50 % binder and air. As a result of the fragility of the part, the part must be first cured generally by placing the build platform inside a furnace at variable periods and temperatures depending on

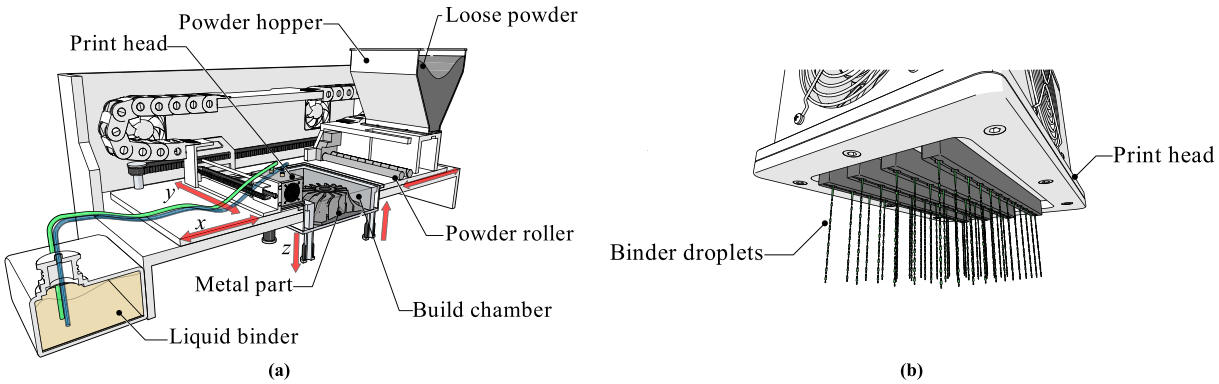

Fig. 5. (a) Schematic of a typical BJ machine (b) BJ print head.

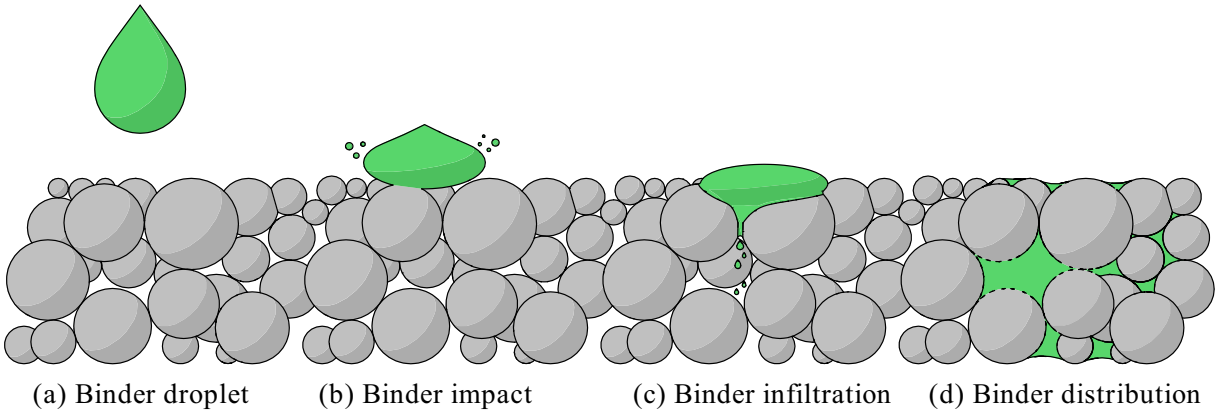

Fig. 6. Schematic of binder droplet morphology.

section thickness, height, excess powder volume, and binding type; though, 6–10 h at a temperature of 200–260 °C is typical. Once cured, the part is extracted from the powder, cleaned, and the excess metal powder is recycled. To improve the mechanical properties of the green metal part, a secondary process is usually undertaken in the form of sintering. Sintering of the green part is performed to reduce porosity, densify, and improve mechanical properties [82].

Sintering is performed in two thermal cycles, usually in an inert atmosphere inside a furnace. First, a de-binding phase is performed where the binder evaporates at temperatures between 175 and 450 °C [77]. The brown part is then subjected to the final cycle, where densification of the porous part occurs at elevated temperatures. The atomic motion during this thermal cycle reduces surface area and surface energy during the increase in temperature from ambient to approximately 80 % of the melting point of the metal [36]. Fig. 7 represents the four stages of sintering. Initially, the density of the part is around 60 % of the theoretical [83], and at lower temperatures, densification is negligible with slight atomic movement and zero shrinkage, as shown in Fig. 7 (i). During the early stage inside the furnace, and as the temperature increases, weak forces pull the particles together by grain boundary and volumetric diffusion [84], fostering mass movement and surface neck growth, leading to 2–3 % densification shown in Fig. 7 (ii) [77]. Then, at the intermediate stage, as furnace temperatures increase, growing necks amalgamate with pores between particles metamorphosing and shrinking into tubular pores conceding to 92–93 % densification of the theoretical shown in Fig. 7 (iii) [77]. Finally, as the maximum temperature within the furnace is reached, tubular pores are reduced as grain growth accelerates, leading to pore isolation at the grain boundaries in Fig. 7 (iv). To achieve this level of densification, sintering in a vacuum is required. Generally, the final sintering volume is less than the original; however, the part's mass remains constant.

When necking begins in the early sintering stage, shrinkages of 1.5–3 % of the green part are typical [77,85]. Several factors, particularly wall thickness, govern shrinkage, and the expectant reduction of smaller components with uniform wall thickness tends to be relatively assured compared to larger components with variable wall thickness. Thus, calculating, regulating, and counteracting shrinkage during the final BJ sintering cycle is a significant limitation compared to other MAM technologies. Although application-dependent, parts can be polished or machined to improve surface finishes. One of the main advantages of binder jetting is its final surface roughness of around Ra 6 μm after post-processing, and tumble polishing can result in finishes of Ra 1.25 μm [36].

6.2. Material characterization of BJ

ExOne manufactures several BJ machines capable of processing various metals. Another is DM, with their Shop System and Production System. Table 11 presents availability from both companies. Table 12 shows the materials currently in development by ExOne and DM, and Tables 13 and 14 compare the mechanical properties for 17–4 PH SS and 316 L SS for the machines.

6.3. Process characteristics of BJ

BJ research is still relatively limited compared to other MAM technologies; however, a significant increase in activity has been underway over the last decade [81]. Most works focused on increasing the diversity of materials that could be printed in addition to microstructural analyses and various ways to achieve part densification. On the other hand, it has been suggested that insufficient research has been done on

Table 11
BJ Commercial material availability [86,87].

Metal categories	Alloy	ExOne	DM shop system	DM production system
Stainless steel	17–4 PH SS	×	×	×
	316 L SS	×	..	×
	304 L SS	×	..	..
Tool steel	M2	×	..	..
Nickel alloy	IN718	×	..	..

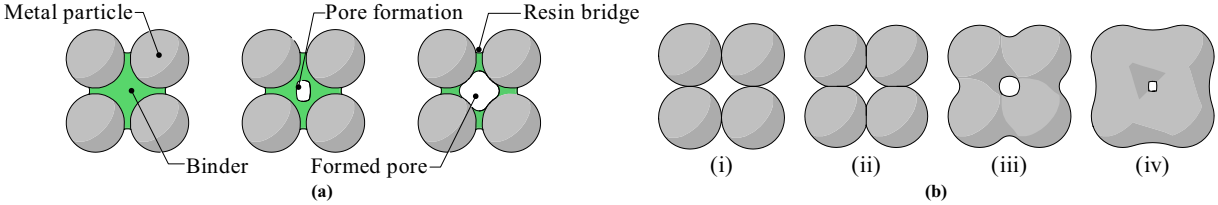

Fig. 7. (a) Schematic of powder particle binding mechanism (b) Four stages of sintering particle densification (i) ambient temperature (ii) Neck growth – initial bonding (iii) Pore rounding – necks merge to form tubular pores (iv) Pore closure – grain growth with closed pores.

Table 12
BJ Research and development materials [86,87].

Metal categories	Alloy	ExOne	DM shop system	DM production system
Stainless steel	420 SS	×	..	×
Tool steel	S7	..	..	×
	M2	×	..	..
	H11	×	..	..
	H13	×	..	×
Low alloy steel	4140	×	..	×
	4605	×	..	..
Nickel alloy	IN625	×	..	×
	IN718	×	..	..
Aluminum	6061	×	..	..
Native metals	Gold	..	..	×
	Silver	..	..	×
	Copper	×	..	..
Copper alloy	Bronze	..	..	..
Titanium	Titanium	×	..	..

characterizing the mechanical properties of printed parts [36]. This observation is also acknowledged in the present review, given the lack of literature regarding the mechanical properties of modern BJ machines. As there was only one study documented above for 17–4 PH SS, this is particularly relevant. Similarly, predicting and controlling the accuracy of the part during printing and sintering because of shrinkage and its influencing mechanisms are still not well understood [97] despite the considerable effort that has already gone into understanding the characteristics of part shrinkage. For instance, the tolerances of some parts can be dictated by how well shrinkage can be controlled, and sintering temperatures may be one of the most influential factors that dictate the degree of shrinkage as opposed to the sintering time or rate [81]. However, sintering time has been shown to influence the density of the green part and has resulted in shrinkages of up to 25 %. Nevertheless, several studies have shown that shrinkage is often very similar horizontally yet higher linearly, partly due to the effect of gravity and partly due to the porosity amid the layers [98]. The weight of each successive layer has been thought to contribute to linear shrinkage, and that distortion during the sintering phase causes differential shrinkage rates due to thermal gradients [36]. It has been suggested that parts can be covered in non-reactive powder, such as alumina, to negate these effects. Another method relates to using reactive binders and nanoparticles. It may also be possible to print parts with consistent shrinkage levels by controlling the porosity by adding fugitive powders (e.g., nylon) [99]. In a similar context, the effects of shrinkage-related distortion have been investigated for parts with complex geometries. For example, it was recently shown that as sintering temperatures are increased, parts can distort by up to 1.0 deg. [99]. On the other hand, other studies have shown opposite effects. A framework for removable dentures was printed by BJ, demonstrating that complex metal structures like this could be printed with minimal deviation from the original CAD model (± 0.5 mm) with consistent shrinkage. These pre-trials uncovered the amount of scaling required to counteract shrinkage, which was 17 % in the x- and y-direction and 19 % in the z-direction. Studies like this demonstrate that although many modern BJ machines can scale parts up to compensate for uniform shrinkage, the nature of shrinkage in some sintered parts is typically non-uniform and one of the most reliable solutions to negate dimensional deviation is to predict the effects of non-uniform linear shrinkage during the design phase. However, much effort is required to forecast this reliably and may depend on the users' experience. Alternatively, an artificial neural network (ANN) based geometric compensation algorithm recently developed exhibited considerable improvements in part accuracy, helping to counteract shrinkage and deformation in DMLS parts [100]. Accordingly, it would be reasonable to suggest that future research and development based on this development would be beneficial to BJ technologies. A summary of the characteristics of shrinkage is given in Table 15. Various other process parameters can also adversely affect quality, such as the BSL, which negatively impacts the homogeneity, mechanical properties, and density of the final part [98]. The formation of the liquid binder droplets inside the inkjet print head is characterized by surface tension and viscosity, with the size of droplets defining the accuracy of the part while BSL determines the overall performance.

For instance, condensed saturation inhibits the proper bonding of the powder particles with the binding agent, reducing the mechanical properties. Conversely, highly concentrated BSL can cause excessive powder accumulation, resulting in geometric deviations; however, quantifying the appropriate BSL can be challenging [102]. Some recent studies comparing experimental and theoretical work have shown that capillary pressure primarily influences the BSL, yet measuring the interaction can be problematic [81]. Recent work has demonstrated the exceptional accuracy and mechanical properties obtained for 316 L SS green parts using novel phenolic binders and low BSL levels (30.2 %) with an LT of 100 μm [103]. However, these novel techniques can also

Table 13
Comparison of mechanical properties of 17–4 PH SS for BJ.

Alloy	Process	Reported by	Machine	Orientation	Condition	UTS, MPa	YS, MPa	El, %	Ref.
17–4 PH SS	Wrought	CES Granta	…	…	H900 Heat-treated	1379	1233.5	15	[64]
	Cast	CES Granta	…	…	H900 Heat-treated	1306.5	1161	4.35	[64]
	MIM	Watson et al.	…	…	As sintered	775–950	675–775	5–7	[44]
	BJ	(*mf*) ExOne	ExOne	Horizontal	H900 Heat-treated	1070–1030	970–1030	4–12	[88]
	BJ	Huber et al.	ExOne Innovent+	Horizontal	As sintered (1300 °C)	1050	…	4.1	[89]
	BJ	(*mf*) DM	Shop system	Horizontal	As sintered	912	660	5.9	[90]
	BJ	(*mf*) DM	Shop system	Horizontal	H900 Heat-treated	1205	981	11.9	[90]
	BJ	(*mf*) DM	Production system	Horizontal	As sintered	900	655	10.9	[91]
	BJ	(*mf*) DM	Production system	Horizontal	H900 Heat-treated	1315	1130	8.4	[91]

Table 14
Comparison of mechanical properties of 316 L SS for BJ.

Alloy	Process	Reported by	Machine	Orientation	Condition	UTS, MPa	YS, MPa	El, %	Ref.
316 L SS	Wrought	CES Granta	…	…	Annealed	522.5	240	40	[64]
	Cast	CES Granta	…	…	Water quenched	552	262	55	[64]
	MIM	Hamidi et al.	…	…	As sintered	410	200	21.8	[92]
	BJ	(*mf*) ExOne	ExOne	Horizontal	H900 Heat-treated	450–580	140–220	40–55	[93]
	BJ	Lecis et al.	ExOne Innovent+	Horizontal	As sintered	534–540	174–176	49–55	[94]
	BJ	Nastac et al.	ExOne Innovent	Horizontal	As sintered	517	214	43	[95]
	BJ	(*mf*)	Production system	Horizontal	As sintered	510	155	75.3	[96]

Table 15
Summary of the characteristics of shrinkage for BJ.

Defect	Cause	Effect	Mitigation	Ref.
Shrinkage	Distortion during sintering due to thermal gradients, the weight of the successive layers (e.g., gravity), and porosity.	Poor dimensional accuracy.	The use of nanoparticles, non-reactive and fugitive binders, compensate for shrinkage during the design phase, ANN.	[36,81,100,101]

produce unique and undesirable results, whereby the surface roughness can increase, and strength can be reduced as the LT increases. Mechanical properties comparable to casting have been obtained for 316 L SS by customizing the BSL in the range of 55–70 % and LT to 50–100 μm. As BSL levels are increased, parts exhibit elevated inhomogeneous properties that intensify as the LT is also increased [94].

Although BJ typically produces isotropic parts that are difficult to achieve with other MAM technologies [36], a comprehensive analysis of all process-structure-property relationships is still necessary to produce reliable parts. Dedicated articles dealing with powder characteristics also mention other important parameters, including particle size distribution and morphology [81]. Nonetheless, one of the most notable challenges for metal binder jetting is the incidence of shrinkage in terms of achieving highly dense metal parts [98]. Compared with other MAM technologies, BJ is highly scalable, it can process multiple materials, and the initial investment is relatively low [101]. If part quality can be reliably controlled, BJ can become a highly integrative manufacturing process in many industries, particularly healthcare and tooling [98]. A summary of the advantages and disadvantages of BJ is presented in Table 16.

7. PBF technology

PBF involves the melting or sintering metal particles together using a thermal heat source. Many variations of PBF exist, and all boast corresponding traits. These include a build chamber with an inert atmosphere to reduce oxidation of the molten metal, a thermal source for fusing metal powder particles, a mechanism to control the fusion, and a method of depositing and smoothing each layer of metal powder. The distinguishing feature of PBF systems is the energy source used, usually a laser or electron beam. Technologies that utilize electron beams are described as EBM processes. Lasers are the most conventional energy source and are typically differentiated by the metal powder particle fusing mechanism, either by laser sintering or laser melting, and are known as SLS and SLM. Depending on whether the laser sinters or melts, the powder particles will ultimately determine the degree of densification of the metal part. For instance, in SLM technologies, the powder is entirely melted into a liquid and then solidified repeatedly and rapidly, promoting homogenous and fully dense parts [104]. In SLS technologies, the powder is not melted but sintered to achieve sufficient surface diffusion of the particles, producing a low-density green part typically with inherent porosity and anisotropic mechanical properties.

Table 16
Summary of the advantages and disadvantages of BJ.

Advantages	Ref.	Disadvantages	Ref.
Low capital cost.	[98]	Porosity.	[76,98]
High scalability potential.	[98]	Difficult to predict and control shrinkage.	[36,81,98,102]
Does not require support structures.	[98]	Complex binder-particle relationship.	[76,98,102]
Relatively high production rate.	[76]		
Relatively good surface finishes	[102]		
Low RS	[81]		

7.1. PBF process

The PBF process illustrated in Fig. 8 shows the inside of an inert (nitrogen or argon gas) build chamber where thin layers of metal powder in the range of 20–200 μm [33] are spread across a powder bed and distributed evenly via a powder spreader, also known as a re-coater. If the re-coater is not adjusted correctly, deformation of the layers, known as 're-coater bump,' can arise, which must be accounted for during the design phase. After the first layer has been deposited and spread, a high-powered beam is used to melt or sinter the powder particles according to a toolpath based on a 3D CAD model. Simultaneously, support structures are built from the same material to mitigate any likely distortion induced by high temperatures during the melting or sintering phase. Following the scanning of the initial layer, the powder bed moves in the negative z-direction equidistant to that of the previous layer, where the powder store and re-coater distribute a subsequent layer of loose powder. This sequence is then repeated until the part is finished. After completion, gradual equilibrium to ambient temperature is observed to avoid thermal shock and allow safe handling. After the part has become stable, it is removed from the powder bed, where the excess loose powder is manually removed and recycled. Because PBF technologies employ distinct particle fusion mechanisms to produce metal parts in the form of melting or sintering; the characteristics of the finished part depend heavily on the cyclic mechanisms involved in the super-rapid melting and solidification of the metal powder with operating temperatures of up to 3000 °C along with higher gradients of ~10^5–10^7 °C/m in the molten pool and heat-affected zone (HAZ) together with cooling rates of between 10^4 and 10^6 °C/s for melting processes [105,106].

In contrast, sintering temperatures are governed by the metal specification, typically below the melting point with cooling rates in the range of 10^5–10^6 °C/s [107]. For melting, high powdered lasers between 200 and 500 W are employed, and the precision is dependent on the beam's diameter, also known as spot size, in the range of 20–500 μm, depending on the machine specifications [51]. Similarly, the LT, typically in the same range as the spot size but relative to the largest powder particle size in the region of 10–60 μm, also defines the tolerance and accuracy of the part [108]. For example, the dynamics of PBF processes, such as the rapid cooling rates that the metal undergoes, call for specific and sophisticated powder morphology characteristics produced through gas or plasma atomization processes which can be relatively expensive. The need for such superior powders for PBF systems is a fundamental issue for the compatibility of commercial metals for these machines. Fine metallic powders used in PBF systems must be treated and stored with care because powder quality can deteriorate due to their susceptibility to absorb various elements in the atmosphere, where contamination can detrimentally influence the final part characteristics. In addition, reprocessing powder and whether it is suitable to reuse is also an important consideration. For instance, powders have been observed to degrade significantly over time. In one study, it was shown that over the course of 30 months of reusing AlSi10Mg powder, significant aging of particles with the potential for detrimental influences on the mechanical properties of parts manufactured with recycled powder [109]. Recycled powder can also affect the mechanical properties of some materials due to changes in proportions and damage to the powder particles [110]. Further, the handling and exposure of fine powders, particularly during powder removal, have been identified as health and safety risks; therefore, decision-makers should consider and budget for these when deciding what MAM technology to implement.

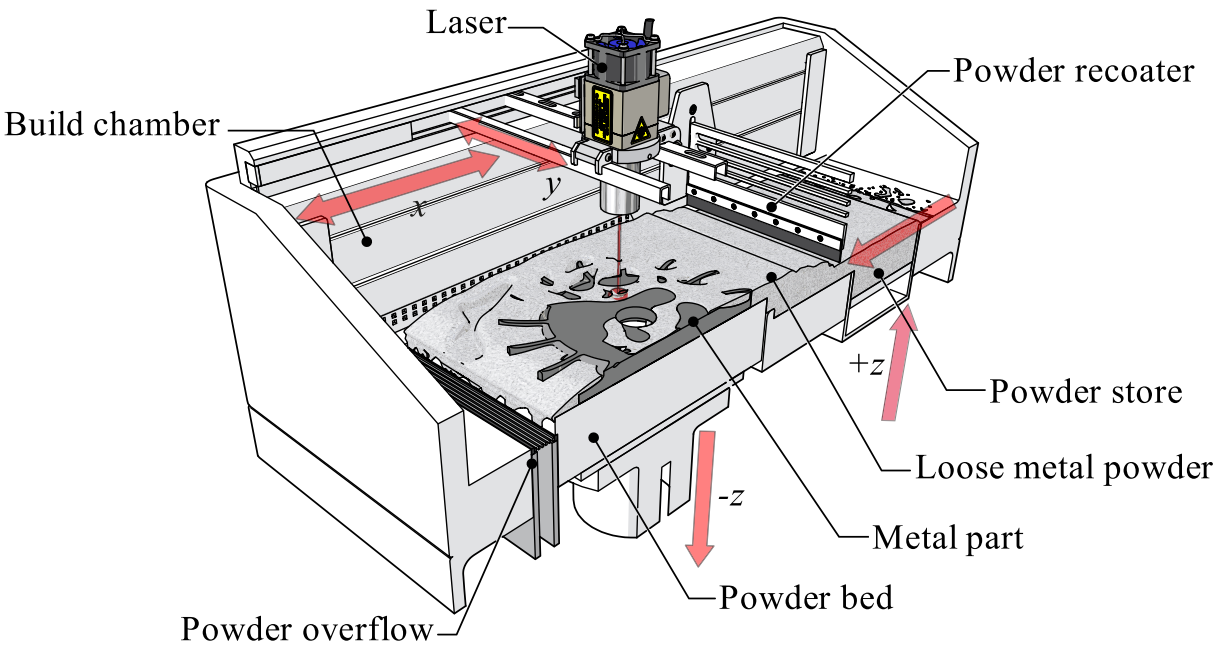

Fig. 8. Schematic of a typical PBF machine.

7.2. Material characterization of PBF

Only 17–4 PH SS, 316 L SS, IN718, and AlSi10Mg will be compared to limit the scope of this article. Table 17 presents commercial material availability based on three machines selected from Table 4: GE M2 Series 5 and EOS M290. These materials are then compared for each machine in Tables 18, 19, 20, 21, and 22.

7.3. Process characteristics of PBF

A great deal of work has been done to characterize PBF processes, and much literature describes what is currently understood and what is still unknown. The following section summarizes some of the most important challenges and techniques that have recently shown promise in improving the quality and reliability of the PBF process. It is estimated that over fifty parameters can affect the final part properties, and they can be classified into three categories: pre-processing, controllable (printing), and post-processing [134]. These parameters can be responsible for some of the main challenges which currently encumber the development of PBF, including repeatability, consistency, and stability of the process, most of which can be attributed to surface roughness, porosity, and RS [135]. Surface roughness can significantly influence fatigue strength by as much as 60 % [136] and affect wear, corrosion resistance, and geometrical accuracy. Among these, surface roughness has been credited as one of the most detrimental factors and can be caused by various incidents such as the stair-stepping effect, adherence of partially melted powders, and unmelted regions of the part [135]. However, its underlying mechanisms have been mainly ascribed to the complex fluid dynamics and solidification process. To elevate these effects, reducing hatch spacing by less than 45 μm and limiting laser power or the scan has been shown to improve surface roughness [19,137]. The angle of incidence of the laser about the platform has also been shown to influence surface roughness, as well as the microstructure of the part and the thickness of the thin walls [138]. This was investigated by a novel method to analyze the relationship and predict its effects. Maintaining a constant angle reduced the surface roughness of an entire part from 19 μm down to 11 μm. Several numerical models have also been trialed recently to predict the effect of surface roughness. For example, a two-tiered numeric model to simulate the behavior of melt pools to understand the development of surface roughness in overhanging regions [139] and an analytical model to predict the upper surface roughness of PBF parts [140]. However, despite these attempts, the root cause of surface roughness could not be sufficiently identified, and a reliable prediction method has yet to be developed [138]. In addition to poor surface finishes, high porosity is another significant challenge that can negatively influence corrosion resistance, fatigue strength, stiffness, mechanical strength, and fracture toughness [135]. Porosity has sometimes been attributed to inadequate laser power resulting in smaller melting pools that are unable to fully fuse powder particles, resulting in pores that have a sphere-like shape. [141]. Several methods have been used to predict and measure porosity. The most widely used strategies to measure porosity include the Archimedes, micrograph-based, and micro-computed tomography methods. While the Archimedes and micrograph-based techniques can quantify LoF defects, both produce different results, especially when using highly porous samples, and the micro-computed tomography method is limited by voxel size [142]. Aside from models like these, several solutions to mitigate LoF and keyhole porosity have been suggested. For instance, optimizing print parameters and strategies such as increasing the size of the fusion zone and employing post-processing treatments such as HIP [143,144]. Despite these efforts, the relationship between process parameters and defects caused by LoF and keyhole porosity remains undeveloped and one of the most urgent research needs today. [145]. In

Table 17
PBF Commercial material availability [111,112].

Metal categories	Alloy	GE M2 Series 5	EOS (M 100, M 290)
Stainless steel	17–4 PH SS	×	×
	316 L SS	×	×
Maraging steel	M300	×	..
Tool steel	H13	..	..
Aluminum	AlSi10Mg	×	×
	A205	×	..
	AlSi7Mg	×	×
Nickel alloy	IN718	×	×
	IN625	×	×
	HX	..	×
Titanium alloy	Ti6Al4V	×	×
	Ti6242	×	..
Cobalt chrome	MP1 (CoCrMo)	×	×
	MP2 (CoCrW)	×	×

Table 18
Comparison of mechanical properties of 17–4 PH SS for PBF.

Alloy	Process	Reported by	Machine	Orientation	Condition	UTS, MPa	YS, MPa	El, %	Ref.
17–4 PH SS	Wrought	CES Granta	…	…	H900 Heat treated	1379	1233.5	15	[64]
	Cast	CES Granta	…	…	H900 Heat treated	1306.5	1161	4.35	[64]
	PBF	(*mf*) GE	GE M2 Series 5	Horizontal	As fabricated	995	715	17.3	[113]
	PBF	(*mf*) GE	GE M2 Series 5	Horizontal	Solution annealed	1440	1315	10.6	[113]
	PBF	(*mf*) EOS	EOS M 290	Vertical	As fabricated	924	861	19.9	[114]
	PBF	(*mf*) EOS	EOS M 290	Horizontal	H900 Heat-treated	1336	1235	14	[114]
	PBF	Nezhadfar et al.	EOS M 290	Vertical	H900 Heat-treated	1375	1300	15	[114]

Table 19
Comparison of mechanical properties of 316 L SS for PBF.

Alloy	Process	Reported by	Machine	Orientation	Condition	UTS, MPa	YS, MPa	El, %	Ref.
316 L SS	Wrought	CES Granta	…	…	Annealed	522.5	240	40	[64]
	Cast	CES Granta	…	…	Water quenched	552	262	55	[64]
	PBF	(*mf*) GE	GE M2 Series 5	Horizontal	As fabricated	695	565	39.5	[115]
	PBF	(*mf*) GE	GE M2 Series 5	Horizontal	Stress relief	700	545	37.5	[115]
	PBF	Byun et al.	GE M2 Series 5	Vertical	As fabricated	593.1	430.8	55.2	[116]
	PBF	Byun et al.	GE M2 Series 5	Vertical	Stress relief	594.7	385.1	57.7	[116]
	PBF	Byun et al.	GE M2 Series 5	Vertical	Solution annealed	584.1	308.2	62.8	[116]
	PBF	(*mf*) EOS	EOS M 290	Horizontal	As fabricated	640	540	40	[117]
	PBF	Riikonen et al.	EOS M 290	All	Stress relief	590	500	46.7	[118]
	PBF	Kong et al.	EOS M 290	Horizontal	As fabricated	751.6	637.9	41.2	[119]
	PBF	Kong et al.	EOS M 290	Horizontal	Heat-treated 1050 °C	672.8	423.8	43.9	[119]
	PBF	Kong et al.	EOS M 290	Horizontal	Heat-treated 1200 °C	683.9	415.7	51.6	[119]

Table 20
Comparison of mechanical properties of Inconel 718 for PBF.

Alloy	Process	Reported by	Machine	Orientation	Condition	UTS, MPa	YS, MPa	El, %	Ref.
IN718	Wrought	CES Granta	…	…	Solution treated	870.55	762.1	42.5	[64]
	Cast	Ni et al.	…	…	Heat-treated	965	550	23	[120]
	PBF	(*mf*) GE	GE M2 Series 5	Horizontal	As fabricated	1060	740	29	[121]
	PBF	(*mf*) GE	GE M2 Series 5	Horizontal	Solution annealed	1495	1305	15	[121]
	PBF	Witkin et al.	GE M2 Series 5	Horizontal	HIP + Heat-treated	1407	1055	21.6	[122]
	PBF	Bean et al.	GE M2 Series 5	Horizontal	HIP + Heat treated	1407	1055	21.6	[123]
	PBF	(*mf*) EOS	EOS M 290	Horizontal	As fabricated	1090	800	25	[124]
	PBF	(*mf*) EOS	EOS M 290	Horizontal	Heat-treated	1505	1240	12	[124]
	PBF	Daňa et al.	EOS M 290	Horizontal	Heat-treated	1440–1475	1253–1278	9–14.6	[125]

Table 21
Comparison of mechanical properties of AlSi10Mg for PBF.

Alloy	Process	Reported by	Machine	Orientation	Condition	UTS, MPa	YS, MPa	El, %	Ref.
AlSi10Mg	Die-Cast	CES Granta	…	…	As fabricated	332.5	164.8	5.47	[64]
	PBF	(*mf*) GE	GE M2 Series 5	Horizontal	As fabricated	460	275	11	[126]
	PBF	(*mf*) GE	GE M2 Series 5	Horizontal	Stress relief	340	230	12.5	[126]
	PBF	(*mf*) EOS	EOS M 290	Horizontal	As fabricated	450	270	10.2	[127]
	PBF	(mf) EOS	EOS M 290	Horizontal	Heat-treated	320	260	11	[127]
	PBF	Zhang et al.	EOS M 290	Horizontal	As fabricated	486–500	294–305	6.4–7.3	[128]
	PBF	Girelli et al.	EOS M 290	Horizontal	As fabricated	452	264	8.6	[129]
	PBF	Girelli et al.	EOS M 290	Horizontal	Heat-treated	332	277	5.8	[129]
	PBF	Baxter et al.	EOS M 290	Horizontal	Heat-treated	386	240	5.5–8.8	[130]

addition to these significant defects, RS is also considered a significant problem that merits urgent scientific investigation. This issue is strongly linked to the limited understanding of the effects of high thermal gradients and the rapid cooling rates during the process [146]. Since RS can significantly affect mechanical properties, especially fatigue resistance and dimensional accuracy, much analytical and numerical work has been done to investigate its fundamental mechanisms concerning process parameters based on the likes of predictive finite element method models [147]. From some of these efforts, the main influential variables responsible for RS have been identified and categorized into three groups: beam parameters (e.g., scan speed, power, and energy input), process conditions, and geometry (e.g., layer thickness, geometry, and base plate temperature) and scan strategy (e.g., raster pattern and interlayer dwell time). Because of this, several methods to mitigate RS have been attempted, such as post-processing (e.g., laser shock peening), thermal control (e.g., preheating the powder bed), scan strategy control (e.g., algorithms), and feedback control (e.g., thermal cameras) [148]. However, it has been demonstrated that some of these mitigation techniques are flawed. For instance, although preheating the powder bed can reduce RS, excessive preheating can have the opposite effect by increasing the risk of grain coarsening of the melt and HAZ zone [146]. It has also been argued that optimizing process parameters has limited effect in alleviating RS, and the most effective solution is to use post-processing techniques such as traditional heat treatments, including HIP [135]. However, while post-processing can relieve RS, these methods are not always economically viable [149]. Overall, the complex

Table 22
Comparison of mechanical properties of Ti6Al4V for PBF.

Alloy	Process	Reported by	Machine	Orientation	Condition	UTS, MPa	YS, MPa	El, %	Ref.
Ti6Al4V	Cast	CES Granta	…	…	Annealed	930.4	839.9	8.99	[64]
	Wrought	CES Granta	…	…	Annealed	918	845.7	11.83	[64]
	PBF	(*mf*) GE	GE M2 Series 5	Horizontal	As fabricated	1295	1145	8	[111]
	PBF	(*mf*) GE	GE M2 Series 5	Horizontal	Stress relief 1	1010	920	15.5	[111]
	PBF	(*mf*) GE	GE M2 Series 5	Vertical	Stress relief 1	1005	915	15	[111]
	PBF	(*mf*) EOS	EOS M 290	Vertical	As fabricated	1075	965	14	[131]
	PBF	(*mf*) EOS	EOS M 290	Horizontal	Heat-treated	1055	945	13	[131]
	PBF	Wang et al.	GE M2 Series 5	…	As fabricated	1191	908	9.2	[132]
	PBF	Wang et al.	GE M2 Series 5	…	Heated treated	1117–1220	863–917	10–12	[132]
	PBF	Ju et al.	EOS M 290	…	As fabricated	1223.5	1128	9.7	[133]
	PBF	Ju et al.	EOS M 290	…	Heat treated	1071.8	892.4	12.8	[133]

characteristics of PBF and the numerous variables involved in optimizing process parameters to reduce or eliminate defects caused by surface roughness, porosity, and RS pose a significant challenge and are computationally inefficient. It is unclear how most of these defects relate to the many variables of PBF and their true nature, according to the most recent literature. The main characteristics of the defects of PBF are given in Table 23.

In-situ sensing and process monitoring have recently increased attention to addressing these issues [151]. Using data from various monitoring and diagnostic sensors to characterize the build process and identify defects in real-time to predict the part's properties in a closed-loop feedback system to control and adjust process parameters autonomously has been recently referred to as 'smart manufacturing' [152]. Currently, a large body of research focusing on various in-situ sensing and process controls has been investigated, and an overview of the most recent achievements in this field can be found in reviews [150,153–155]. Ultrasonic testing, acoustic and optical emission spectroscopy, optical and x-ray tomography, pyrometry, and infrared imaging have all been used for in-situ monitoring. Many PBF manufacturers also offer proprietary modules that can be retrofitted to legacy machines incorporating one or more sensors, although data can only typically be analyzed retrospectively. Despite the progress in gathering information in this way, it is evident that the main challenge in developing a closed-loop intelligent system to correct defects in real-time is processing and identifying patterns between large amounts of sensor data and process parameters. Recent developments in machine learning (ML) algorithms have proven to be a capable method of pattern recognition and anomaly detection of multiple sensor signals to deal with this issue. Several valuable reviews on ML for AM applications can be found in [156–158].

While ML is currently in development, there remains significant scope for improved data handling. At the same time, computational cost, qualification standards, and data acquisition techniques will all need to be addressed before ML, and AM is properly integrated into a closed-loop system [159]. Combining MAM with traditional post-processing techniques, e.g., milling, turning, deformation, vibration, and heat treatments in an integrated manufacturing system, has also been explored to address defects. This combination is termed HAM and is defined as 'the controlled application of process mechanisms on additively deposited materials and the controlled application of AM on primarily processed raw materials previously subjected to TM processes' [160]. Several HAM machines are sold commercially, along with a handful of PBF-HAM machines listed in Table 24.

Only a relatively modest amount of work has been done to characterize PBF-HAM, primarily due to the difficulty of incorporating subtractive processes with a powder bed, limited availability of commercial PBF-HAM machines, technological barriers to combining PBF and post-processing processes, and only a subgroup of applications require superior surface finishes and dimensional accuracy [167]. Nevertheless, a few studies are found in the literature concerning the mechanical properties of the machines mentioned in the above table. The results from these papers are summarized in Table 25.

Other findings involving PBF-HAM have also been reviewed recently [171–173]. Studies show that the main advantages are improved surface roughness, dimensional accuracy, improved part distortion, relieving RS, reducing human error, and reduced lead times and material waste. Because MAM and TM have their own unique advantages, the amalgamation of both technologies presents integral manufacturing and economic advantages resulting from a decentralized process cable of producing intricate and functional metallic parts that are difficult to produce by standalone processes. On the other hand, despite the benefits of PBF-HAM, many issues still need to be resolved in understanding additive technologies and their interface with post-processing methods as a single system before the full implementation of hybrid machines can be realized. For instance, there is insufficient research on processing hard-to-machine materials such as superalloys, and thus the variety of materials that PBF-HAM machines can process is limited [172]. Recent work demonstrated the impact of cutting fluid for HAM milling and found that high oil concentrations lead to hydrogen-induced cracking [165]. Although this study was carried out using DED-HAM, the effects on PBF systems can be even more detrimental due to the presence of the powder bed and the potential for fluid to impair or influence its characteristics. Several other issues related to the implementation of HAM are also noted in the literature, such as the geometric uncertainty of the MAM process, powder recycling, and recovery and protection of machining components from fine powder particles.

Moreover, besides understanding the principles and nuances of MAM and post-processing techniques separately, engineers and operators must also be aware of hybrid systems' capabilities and potential issues. However, the lack of knowledge of the hybrid process may hinder the technology's wider adoption. On the other hand, there is an opportunity for much research besides developing a novel methodology (similar to DfAM) for designing metal parts by HAM which is currently non-existent. Despite its popularity, PBF remains an imperfect solution. The limitations mentioned above (e.g., poor surface finishes, porosity, and RS) may impede the current likelihood of processing mass-produced metal parts reliably and repeatably. Nevertheless, the present and future interdisciplinary efforts between materials science and information technology will likely resolve these issues as the body of research continues to expand. A summary of the advantages and disadvantages of PBF is presented in Table 26.

8. DED technology

DED is a process that uses a focused thermal energy source to melt material as it is deposited by a nozzle, similar to the principles of welding [5]. The DED process is typically suited to creating near-net-shaped parts and repairing or adding features to existing components and shares 16 % of the total MAM market [55]. Many variations of DED exist; however, the following sections will focus on selecting the most popular machines today. Although a brief overview of the DED process is described next, a comprehensive explanation for each DED process can

Table 23
Summary of the main characteristics of PBF defects.

Defect	Cause	Effect	Evaluation	Mitigation	Ref.
High surface roughness	The stair-stepping effect, adherence of partially melted powders to the surface of the metal and un-melted regions of the part, rapid solidification, variable powder particle sizes, and high laser scanning speeds.	Reduced fatigue strength, wear, and corrosion resistance Poor geometrical accuracy.	Profilometry, optical tomography.	Larger spot sizes, uniform powder and spreading, limiting laser power or the scan speed, post-processing/HAM.	[19,135,144,150]
Porosity	LoF, gas entrapment, balling effect, poor wetting, high overlapping ratio, dense powder packing, and high laser energy density.	Reduced corrosion resistance, fatigue strength, stiffness, mechanical strength, and fracture toughness.	Archimedes method, X-ray tomography, pyrometry, ultrasonic testing, optical emission spectroscopy (OES), and transient thermos-reflectance (TTR).	Finer and more spherical powder particles, preheating the substrate, uniform gas flow rate across the build area. Post-processing/HAM.	[135,144,150]
Residual stress	High thermal gradients and rapid cooling.	Reduced fatigue performance and mechanical properties, poor geometrical accuracy.	Numerical modeling, Barkhausen noise, X-ray diffraction, hole drilling, spot annealing, thermomechanical, thermal modeling.	Post-processing/HAM, preheating the substrate, thermal control, scan strategy control, feedback control IR cameras.	[135,148,150]

be found in Gibson et al. [35].

8.1. DED process

The DED process illustrated in Fig. 9 (a) uses a heat source (b) capable of fully melting a feedstock (wire or powder) into a melt pool [174]. Four thermal energy sources are typically used in DED technologies: plasma laser, electron beam, electric arc, and laser beam. The metal part is generally created or repaired inside a hermetically sealed build chamber on a build plate. The feedstock is targeted toward the energy source by either blowing powder (spherical particles in the range of 50–200 μm) toward the metal part via a coaxial nozzle or by pushing or feeding a metal wire (in the range of 1–3 mm in diameter) via a delivery nozzle. The feedstock melts on contact with the energy source, prompting it to drip or spray into a melt pool of typically 0.25–1 mm in diameter and at a depth of 0.1–0.5 mm [35].

Metal particle fusion mechanisms vary between each DED technology. For instance, in powder-type systems, the metal powder arrives at a melt pool of material, initially fuses, and then melts to join the melt pool, cools, and solidifies. In wire-type systems, the wire softens and binds to the previous layer, solidifying at a rate of 10^3–10^5 °C/s [35]. The nozzle and feedstock move the melt pool along a pre-set toolpath, and a CNC robotic arm typically controls the movement of the nozzle and feedstock in conjunction with a build plate which is sometimes attached to a turntable. As the nozzle and feedstock move away from the melt pool, the material solidifies, and the process continues along the remaining toolpath building up intersecting paths until the part is complete.

Each intersecting path is typically 25 % of the pathwidth with a typical LT of 0.25–0.5 mm [35]. The fusion mechanism mimics conventional welding processes where a significant concentration of energy is required to sustain the melt pool and fuse each path and the ensuing layers. Similarly, a HAZ, which surrounds the melt pool, is exposed to intense thermal gradients that generate high RS [175–177]. When stresses entrapped within a part are abruptly released, cracks may develop due to the rapid cooling rates negatively influencing the grain structure, performance, and lifespan. RS can be relieved partway through the build by removing the part and heat-treating it inside a furnace for a period before continuing with the build. Additional limitations of DED are the low geometric accuracy of printed parts where tolerances of less than 0.25 mm and surface roughness of less than 25 μm are typical. However, tolerances and surface finishes are print speed-dependent—the higher the print speed, the lower the accuracy [35].

Conversely, slower print speeds enhance the surface quality of finished parts. Due to the large melt pools created by the high thermal energy, intricate interior geometries and overhanging supports are challenging to process. Hence, striking a cost-effective balance between productivity and part quality involves optimizing the process parameters. On the other hand, DED offers many advantages over other MAM technologies. For instance, DED systems can process many commercial welding and powder metallurgy materials. DED can also create fully dense parts with single-crystal structures where the microstructure can be tailored because of the process's unique ability to accommodate several materials into a single build besides controlling the solidification rate of the deposited material. An investigation by Optomec [178] found that their DED process was 20 times faster than the PBF, taking 240 h to complete and costing 16,800 USD, while the Optomec LENS 850R DED took 13 h at the cost of 3200 USD. The abundance, affordability, and convenience of wire and powder feedstock materials used for DED machines and high printing speeds give rise to a relatively economical process. Due to the high buy-to-fly ratio of most TM processes, DED is considered an ideal substitute. For instance, The Welding Institute (TWI) manufactured a helicopter combustion engine chamber by DED and found that the overall density was roughly 99.5 % with a 70 % powder efficiency, and the fly-to-buy ratio was less than what would be expected from machining. Moreover, the estimated machining time of 2 months was reduced to only 4.5 h [179,180].

Table 24
Commercially available PBF-HAM machines.

Manufacturer	Machine	MAM process	Post-process	Hybrid combination	Max. work size, mm	Country	Ref.
Matsuura	Lumex Avance-25	SLM	Milling	SLM + milling	256 × 256 × 185	JP	[161]
Matsuura	Lumex Avance-60	SLM	Milling	SLM + milling	600 × 600 × 500	JP	[162]
Sodick	OPM250L	SLM	Milling	SLM + milling	250 × 250 × 250	JP	[163]
Sodick	OPM350L	SLM	Milling	SLM + milling	350 × 350 × 350	JP	[164]
HBD3D	HBD-280F	SLM	Milling	SLM + milling	250 × 250 × 300	CN	[165]
Additive Industries	MetalFAB2	SLM	Heat treatment	SLM + heat treatment	420 × 420 × 400	NL	[166]

Table 25
Mechanical properties of commercial PBF-HAM machines.

Alloy	Process	Reported by	Manufacturer	Machine	UTS, MPa	YS, MPa	% El, %	Ra, μm	Ref.
18Ni-300 MS	PBF-HAM	Mutua et al.	Matsuura	Lumex Avance-25	1125	300	10.4	35	[168]
18Ni-300 MS	PBF-HAM	Sarafan et al.	Matsuura	Lumex Avance-25	1171	1062	12.9	0.32–0.80	[169]
AISI 420	PBF-HAM	Shen et al.	Sodick	OPM250L	829.8–1541	481.1–1005	1.17–1.83	…	[170]

Table 26
Summary of the advantages and disadvantages of PBF.

Advantages	Ref.	Disadvantages	Ref.
Relatively high accuracy.	[171,173]	Relatively poor surface finishes.	[138,150,171]
Near net-shaped production.	[135]	Relatively high porosity.	[135,141,150]
High material utilization fraction.	[135,173]	High residual stress.	[141,148,171]
High specific strength and stiffness.	[171]	Typically requires post-processing.	[141,171]
Ability to recycle powder.	[171]	Support structures are required.	[141,171]
High geometrical complexity.	[171–173]	Powder handling health and safety issues.	[171]
A broad range of feedstock materials.		Low productivity.	[171,172]
		Limitations on build envelop.	[171,172]
		Complex process-property relationship.	[134,141]

8.2. Material characterization of DED

Many 'off-the-shelf' materials can be used with DED, especially those meant for welding and powder metallurgy. The following section focuses on the performance of three systems shown in Table 27 and Tables 28–32 compares the mechanical properties against wrought and cast counterparts.

8.3. Process characteristics of DED

Much of the literature on DED discusses the correlation of the process-structure-property-relationship, and many of the defects that arise during the process are similar to the characteristics of other MAM processes, especially PBF. However, its adoption has been limited, primarily due to several defects that have not been sufficiently characterized [185]. These include RS, cracking and delamination, porosity, and high surface roughness [35,188] and are listed in Table 33, including their origin, effects, and likely mitigation techniques. As such, this section will explore the characteristics of DED to a limited degree.

One of the main advantages of DED is its ability to produce large components, which has recently been considered for the construction industry. However, while DED technology has the potential to be used in many of these areas, it is currently suited for structures that are smaller than those typically encountered in the construction industry [186]. On the other hand, and as we have already noted, a printed metal bridge was manufactured over six months by MX3D using WAAM technology [10]. To accomplish something of this magnitude, comprehensive testing was conducted, including a stub column assessment, and a variety of geometric measurement techniques were utilized because of the disparity in wall thickness, including calipers, tomography, digital image correlation, and 3D laser scanning; however, the Archimedes method was deemed the most reliable method. Being the first of its kind and outside the scope of standardized design codes, and having uncharacteristic mechanical properties, numerical models using nonlinear FEA methods were developed to understand the structural response and load-bearing capacity. When used together, both the physical and numeric verification methods successfully demonstrated the structure's functional ability.

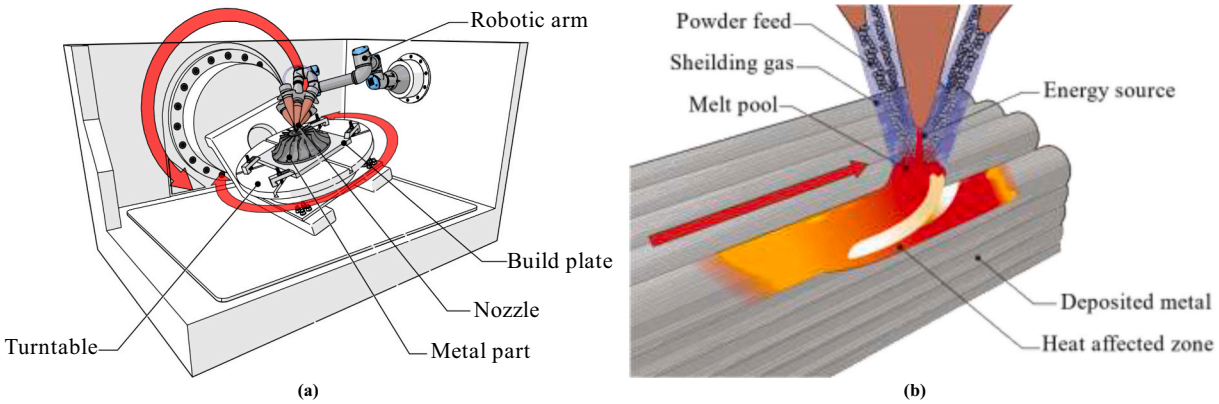

Fig. 9. (a) Schematic of a typical DED machine (b) Typical powder DED fusion mechanism with melt pool and heat-affected zone schematic.

Table 27
DED commercial material availability [52,181,182].

Metal categories	Alloy	Meltio M450	Optomec CS 250	DMG Mori Lasertech 65 DED
Stainless steel	304 L SS	×	…	…
	304 SS	…	×	…
	316 L SS	×	…	×
	316 SS	…	×	…
	17–4 PH SS	…	×	×
	13–8 SS	…	×	…
	410 SS	…	×	…
	308 L SS	×	…	…
Carbon steel	42CrMo4	×	…	…
	10MnSi7	×	…	…
Titanium alloy	Ti6Al4V	×	×	…
	Ti6242	…	×	…
Nickel alloy	IN718	×	×	×
	IN625	×	×	×
Aluminum	4047	…	×	…
Copper alloy	CuSn10	…	…	×
	CuAl10	…	…	×
Tool steel	X35CrMoMn7–2	…	…	×

Apart from this example, WAAM has become well-established in industry, especially aviation. Using parts manufactured by WAAM, Boeing improved its EE and reduced its overall expenditures by 30 %, including a 75 % reduction in manufacturing time [187]. With DED, it is possible to deposit the material directly on an existing surface during the manufacturing process, and changing feedstock materials part way through printing is also possible. Because of these features, one of the main applications for DED is the repair and remanufacturing (RR) of existing components [53]. Compared with other repair processes, such as TIG or plasma transferred arc welding, DED is more efficient due to its lower heat input, reduced distortions, and higher precision. Furthermore, using the DED could result in significant savings in terms of time and cost [53]. However, the characteristics of repairing components using WAAM are still not fully understood, despite the possibility of achieving positive economic benefits [187].

Exploring the implications of process monitoring and control to improve the quality of printed metal parts through process optimization has been investigated recently to help understand the underlying mechanisms responsible for some of the above defects [188]. For instance, in-situ monitoring and thermo-mechanical analysis have been considered for predicting, optimizing, and controlling process parameters in real-time. The current challenges that these technologies would likely relate to are counteracting porosity typical for DED and, like the

Table 28
Comparison of mechanical properties of 316 L SS for Meltio and DMG Mori Lasertech 65 DED machines (average values).

Alloy	Process	Reported by	Machine	Orientation	Condition	UTS, MPa	YS, MPa	El, %	Ref.
316 L SS	Wrought	CES Granta	…	…	Annealed	522.5	240	40	[64]
	Cast	CES Granta	…	…	Water quenched	552	262	55	[64]
	DED	(*mf*) Meltio	…	…	…	642.5	385	49	[183]
	DED	(*mf*) DMG Mori	…	…	As printed	563	390	36.6	[182]

Table 29
Comparison of mechanical properties of 17–4 PH SS for DMG Mori Lasertech 65 DED against wrought (average values).

Alloy	Process	Reported by	Machine	Orientation	Condition	UTS, MPa	YS, MPa	El, %	Ref.
17–4 PH SS	Wrought	CES Granta	…	…	H900 Heat-treated	1379	1233.5	15	[64]
	Cast	CES Granta	…	…	H900 Heat-treated	1306.5	1161	4.35	[64]
	DED	(*mf*) DMG Mori	Laser	…	Age hardened	1134	1053	7.6	[182]

Table 30
Comparison of mechanical properties of Ti6Al4V for Meltio M450 and Optomec CS 250 machines (average values).

Alloy	Process	Reported by	Machine	Orientation	Condition	UTS, MPa	YS, MPa	El, %	Ref.
Ti6Al4V	Cast	CES Granta	…	…	Annealed	930.4	839.9	8.99	[64]
	Wrought	CES Granta	…	…	Annealed	918	845.7	11.83	[64]
	DED	(*mf*) Meltio	…	…	…	950	882	12	[184]
	LENS	(*mf*) Optomec	…	…	…	1077	973	11	[181]

Table 31
Comparison of mechanical properties of IN718 for Meltio M450 and DMG Mori Lasertech 65 DED machines (average values).

Alloy	Process	Reported by	Machine	Orientation	Condition	UTS, MPa	YS, MPa	El, %	Ref.
IN718	Wrought	CES Granta	…	…	Solution treated	869.4	761.2	41.83	[64]
	Wrought	CES Granta	…	…	Solution treated, aged	1246	1051	12.25	[64]
	DED	(*mf*) Meltio	…	…	…	1271.5	1084	7.55	[184]
	DED	(*mf*) DMG Mori	…	…	Age hardened	1268	1089	17.7	[182]

Table 32
Comparison of mechanical properties of IN625 for Optomec CS 250 and DMG Mori Lasertech 65 DED machines (average values).

Alloy	Process	Reported by	Machine	Orientation	Condition	UTS, MPa	YS, MPa	El, %	Ref.
IN625	Wrought	CES Granta	…	…	Annealed	855.8	398	32.34	[64]
	LENS	(*mf*) Optomec	…	…	…	938	584	38	[181]
	DED	(*mf*) DMG Mori	…	…	As printed	844	538	28.9	[182]

Table 33
Summary of the main characteristics of DED defects.

Defect	Cause	Effect	Evaluation	Mitigation	Ref.
Residual stress	High thermal gradients and rapid cooling.	Fractures under stress reduced fatigue performance and mechanical properties.	X-ray diffraction, numerical and thermomechanical modeling, hole drilling, neutron diffraction, Barkhausen noise.	Reduced scan speed, substrate preheating, substrate clamping, inter-pass rolling, LSP, UIT.	[189–191]
Porosity	LoF, Gas entrapment, keyhole mode melting, alloy evaporation, incomplete powder melting, and high laser energy density.	Reduced fatigue performance and mechanical properties, reduced corrosion resistance, and anisotropy.	X-ray tomography, gas pyrometry, Archimedes method, TTR.	Higher thermal input, use of plasma rotate electrode process for powders, post-processing/HAM, uniform gas flow rate across the build area.	[185,191,192]
Cracking and delamination	High thermal gradients and rapid cooling, variable energy input, material property difference between layer interfaces, and the temperature differential between layers.	Fracture under stress reduced fatigue performance, mechanical properties, and corrosion resistance.	Metallographic cross sections, crack opening, and fractography in SEM; NDT: magnetic particles, radiography, I-CT, ultrasonic, computational modeling.	Substrate preheating, regulate the cooling rate, reduce the formation of inter-metallics, and suitable heat transfer channel.	[185,191]
High surface roughness	Low heat input, variable powder particle sizes, high laser scanning speeds, differential cooling, part design, dissimilar weld track.	Reduced fatigue performance and mechanical properties, poor tolerances.	Profilometry, optical tomography.	Gradual stepwise changes in space, increased heat input, reduced layer thickness, finer powder particles, post-processing/HAM.	[185,191]

characteristics of defects in metal PBF parts, is similarly caused by keyholes, gas entrapment, and LoF. Although cracking and delamination are inherent in most MAM processes, DED processes can amplify the effects due to particularized and extreme thermal gradients. Despite this, techniques such as preheating the build chamber, appropriate design intent (e.g., part orientation, limiting wall thickness and aspect ratios), and controlling cooling rates can mitigate cracking. Poor surface finishes are also discussed and attributed to unmelted powder particles, the stair-stepping effect, the spraying of molten metal, and several other less cited factors, such as the poor design and feedstock condition. To improve part resolution, it is recommended that the temperature of the thermal heat source be increased, and print speeds should be reduced. Another technique to mitigate these issues would be using DED-HAM systems [188].

The amount of research and development into DED-HAM systems significantly outweighs any other hybrid combination for other MAM technologies. Among the many configurations that combine DED with the material removal or forming process, DED + machining has had the most attention [193]. This present work has already discussed many of the nuances of HAM in the previous chapter on PBF, and these limitations and research opportunities are equally relevant to DED. Compared to other MAM technologies, DED-HAM is relatively advanced, and as such, a wide variety of commercial systems are available; some of these machines are listed in Table 34. Despite this, very little work has been done to characterize parts manufactured by the commercial machines shown in the above table. Consequently, it is uncertain what impact these machines have on the properties of the final part and correcting defects; however, this presents the opportunity for much research to be conducted in this area. Several studies have been published for other hybrid technologies, and experimental attempts are shown in Table 35. The benefits of DED-HAM include eliminating positioning errors when transferring the part from an additive to a subtractive process. The movement of material around the shop floor can be reduced, which lessens the amount of floor space a factory requires, and capital expenditure for machinery also diminishes, thereby reducing the product's final cost.

The simplicity of controlling only one process is also a distinct advantage of employing a hybridized system [193]. However, the complex interactions of two different manufacturing processes and the need to program intricate tool paths require the skill and knowledge of well-trained and experienced operators. As the most common materials used tend to be hard-to-machine alloys, the machinability of materials is also one of the most fundamental challenges to the broader implementation of HAM, including controlling the dimensional accuracy [171]. For instance, during secondary processes such as CNC milling, the tooling may encounter unexpected material due to deformation or distortion during the printing process, leading to tool damage. On the other hand, in-situ monitoring and inspection techniques could be developed to identify that the physical part has deviated from the original 3D CAD model and account for this before damage occurs [172]. Several other limitations in the literature are summarized in Table 36.

Despite its limitations, the repair capabilities are among the most promising areas for future development opportunities in DED research. Because of the high deposition rates, DED is also the most economical alternative for manufacturing large metal parts [208]. Although research on DED has steadily increased in recent years, especially relating to monitoring and control in addition to DED-HAM for resolving defects, there is also a great need to fully understand the relationship between process parameters and part quality [53]. The advantages and disadvantages of DED from the literature are summarized in Table 37.

9. MAM sustainability

Rising temperatures have been attributed to industrial practices, which account for 15 % of global energy consumption and roughly

Table 34
Commercially available DED-HAM machines.

Manufacturer	Machine	MAM process	Post-process	Hybrid combination	Max. work size, mm	Country	Ref.
DMG MORI	LASERTEC 65 3D	DED	Milling	DED + milling	735 × 650 × 560	UK	[53,171]
DMG MORI	LASERTEC 125 3D	DED	Milling	DED + milling	1335 × 1250 × 900	UK	[53]
DMG MORI	LASERTEC 6600	DED	Milling	DED + milling	1040 × 610 × 3890	UK	[194]
Yamazaki Mazak	Integrex i-400 AM	DLD	Milling	DLD + milling	Ø658 × 1619	JP	[171]
Yamazaki Mazak	Variaxis j-600 AM	WAAM	Milling	WAAM + milling	Ø730 × 460	JP	[193]
Yamazaki Mazak	VC500A/5x	DED	Milling	DED + milling	Ø600 × 306	JP	[195]
OPTOMEC	LENS 500 MTS	LENS	Milling	LENS + milling	500 × 325 × 500	US	[193]
OPTOMEC	LENS 860 MTS	LENS	Milling	LENS + milling	598 × 600 × 610	US	[193]
Hamuel	HSTM 1000 Hybrid	DMD	Turning/milling	DMD + turning/milling	1000	DE	[193]
Okuma	MU-8000 V LASER EX	LMD	Turning/milling	LMD + Turning/milling	Ø1000 × 550	US	[193]
Romi	D Series	DED	Turning/milling	DED + Turning/milling	Varies	BR	[196]

Table 35
Mechanical properties of DED-HAM machines.

Alloy	Process	Reported by	Commercial/experimental	UTS, MPa	YS, MPa	% El, %	Ra, μm	Ref.
316 L SS	DED + milling	Yang et al.	Dalian Sunlight	686.3	483.3	47.1	…	[197]
316 L SS	DED + milling	Feldhausen	Yamazaki Mazak	~610	~400	~51	…	[198]
Bainite steel	DED + HDMR	Fu et al.	Experimental	1275–1309	..	…	…	[199]
316 L SS	DED + hot forging	Duarte et al.	Experimental	622	450	28	…	[200]
Ti-6Al-4 V	WAAM forged +heat treated	Bambach et al.	Experimental	934	850	8	…	[201]
Ti-6Al-4 V	DED + hot forging	Hemes et al.	Experimental	912–916	838–840	13.1–14.5	…	[202]
IN718	WAAM + Interpass rolling	Xu et al.	Experimental	1351	…	…	…	[203]
Al-Mg4.5Mn	WAAM + Interpass rolling	Gu et al.	Experimental	300–344	170–240	20–22	…	[204]

Table 36
Advantages and disadvantages of HAM.

Advantages	Ref.	Disadvantages	Ref.
Improved surface finish.	[160,171,205]	Challenging to process hard-to-machine materials.	[171,172]
Reduced RS.	[171]	Uncertainty of geometric deviation of the additive process.	[171,206]
Improve dimensional accuracy.	[193,205]	Lack of knowledge for process optimization.	[171]
Improved mechanical properties.	[160,193,205]	Cutting fluid can lead to hydrogen-induced cracking.	[171,207]
Heat and surface treatments can reduce porosity.	[160,171]	Cutting chips can affect the process.	[172]
Condensed manufacturing operation.	[193]	Lack of hermetic enclosure can cause powder oxidation.	[171]
Improved productivity.	[171]	Challenging to position complex geometries for secondary processes.	[171]
Elimination of part positioning errors.	[193]	Training of operators is more complex.	[171]
Manufacture of complex parts.	[160,193,205]	Can require advanced process planning.	[172,205]
Reduced overall capital cost.	[193]		
Can reduce overall manufacturing cost.	[160]		
Can reduce material waste.	[160]		

Table 37
Main advantages and disadvantages of DED.

Advantages	Ref.	Disadvantages	Ref.
Can manufacture relatively large components.	[53,174,191]	High residual stress.	[174,191] [209]
Can add material to existing surfaces (repair).	[53,174,191] [209]	Distortion due to high residual stress.	[174,191]
Can process a broad range of materials.	[174,191]	High surface roughness for blown powder machines.	[174,191]
High deposition and build rates.	[174,191] [209]	Post-processing is typically required.	[191]
Part characteristics can be adjusted locally.	[191]	Controlling the process can be challenging.	[209]
Can produce fully dense parts.	[174]		
Ability to change material during the build.	[53] [209]		
Potentially more economical to repair high-value parts.	[53]		

35–40 % of material consumption [210], and the activities responsible for processing metals and alloys are some of the most energy-intensive [211]. Among these, the iron and steel industry accounted for 8 % of global energy consumption, 7 % of all GHGs, and roughly 11 % of all CO_2 emissions [212,213]. Similarly, the aluminum industry accounts for almost another 2 % of total global CO_2 emissions [214]. It has been estimated that current emissions need to be reduced by 45 % by 2030 and reach net zero by 2050 [215], and with many metal manufacturers already working toward these targets, the MAM sector must also commit to safeguarding the environment. According to some [216], the environmental benefits of AM are clear because, unlike FM and SM processes, NNS parts can be created with minimal waste, giving rise to a process that is both resource and EE. By applying DfAM methodologies to optimize the distribution of material for specific loads and boundary conditions to satisfy the required structural performance of a product, the areas of the part that are not supporting the functional loads and not undergoing substantial deformation and thus not contributing to the overall integrity of the component can be removed. For instance, by using topology optimization and by changing the material, the mass of a hinge bracket used on the Airbus A320 was reduced from 918 g to 326 g (50 % material removal and 50 % material change) and compared to the original design, the stress distribution was more homogenous [217]. By depositing material in layers, optimized additive structures, which are typically characterized by complex geometric shapes, can be created

with ease, which means not only is less material required, which significantly decreases the mass of the product, build times can also be reduced, meaning only enough energy per part is needed which has been shown to have positive net environmental implications. As an example, for each kg of material removed from aerospace components, 90,000 l of fuel can be saved, preventing the emission of approximately 230 tons of carbon dioxide into the atmosphere. [218]. Part consolidation has also been emphasized in the literature as one of the most beneficial advantages of AM [219]. In terms of sustainability, an LCA study recently demonstrated that consolidation of a multipart assembly could reduce environmental indicators by nearly 20 % compared with traditional assembly methods [220]. Despite the interest in part consolidation for improved sustainability, only a handful of studies have attempted to quantify its environmental implications. On the other hand, as noted earlier in this article, GE made some significant gains when they consolidated their GE9X engine assembly.

The RR of metal parts has also been shown to reduce a product's overall environmental burden by extending the lifespan of damaged or decommissioned parts [221]. As noted earlier in this review, DED technologies are particularly suitable for RR, and it has been demonstrated that repairing automotive steel dies by DED can restore them to their original condition [222]. A traditionally repaired die had a life expectancy of 12.5–29.2 % of its original state, indicating that the DED repair process was the more sustainable option in the long run. Other avenues have also been explored for energy-saving opportunities. As an example, reducing print times can be a highly effective policy whereby reducing the part's height and minimizing support material, especially for ME technologies, can significantly improve EE. [223]. Additionally, by properly evaluating the design and investigating alternative materials, the overall environmental impact of a product can be dramatically reduced. For instance, by using FEA to analyze the design of vehicle door hinges, it was shown that by substituting steel for aluminum, the overall mass could be reduced by 65 % while maintaining the structural integrity of the component [224]. Similarly, recent LCA studies have also demonstrated that by replacing materials for various components of a vehicle, the overall environmental impact can be reduced by 7–14 % [225]. Although these methods do not relate directly to MAM's functionality, they demonstrate that more sustainable products can be manufactured by reconsidering the choice of material and, if combined with other DfAM techniques, could significantly reduce a product's environmental impact. Thus, the opportunity exists to examine the various combinations of DfAM methodologies for MAM to determine their collective impact. For instance, the configurations in Table 38 could be studied.

Although the methodologies above have shown some environmental benefits, it has not yet been demonstrated sufficiently that the entire MAM process is more sustainable than TM [216]. Indeed, before printing, feedstocks and powders have already undergone a high degree of processing, and without truly knowing the extent to which these consumables and indeed how all other processes in the life cycle impact the environment, direct comparisons with TM processes cannot be made, making its future implications for sustainable manufacturing unclear. For instance, raw material still needs to be extracted and processed into metal ingots, then melted and atomized into fine spherical particles, typically by high-pressure and inert gas streams or liquid streams. Powders then need sieving, washing, drying, reducing, annealing, crushing, transforming, and packaging for commercial sale. Then, depending on the size and complexity of a design, the amount of time needed to print a part can take a few hours to several days, and then some MAM technologies may require additional processing, such as debinding and sintering. In nearly all cases, a post-processing treatment is also needed, such as machining or heat treating, further adding to the overall energy burden of the whole cycle. To add to this, recycling or end-of-life requires consideration, as-well-as transportation. Thus, to quantify and assess the total environmental impact, all inputs and outputs in the cycle should be studied, which can be achieved through an LCA [226]. An example of the various phases for a product manufactured by MAM is illustrated in Fig. 10.

Table 38
Possible combinations for DfAM studies for sustainability.

Method 1		Method 2		Method 3
Topology optimization	and	Material optimization		
Part consolidation	and	Material optimization		
Topology optimization (parts)	and	Part consolidation (assembly)	and	Material optimization

As far as environmental impact assessments on AM are concerned, most of the existing knowledge focuses on polymers, and only a small number of those studies adopt a cradle-to-grave approach. Literature concerning some life cycle phases shows significant gaps, but more importantly, current LCAs are mainly generalized models based on approximations [227]. In part, this is because there is a lack of useable or applicable data, and what exists is ambiguous [228]. Aside from this, most work to date only characterizes the EE of the manufacturing process (i.e., printing). Most studies use the metric of SEC, typically in MJ or kWh per kg of printed metal. Recently, it was shown that MAM processes consume significantly more energy, in the range of 289.75 kWh/kg, whereas the range for combined TM processes was 22.97 kWh/kg [229]. Fig. 11 illustrates the range of SEC for various MAM and TM manufacturing processes. It is worth noting that studies relating to the EE of metal ME technology are missing from the literature, and most other studies were performed with relatively old machines. Thus, it would be worthwhile if future analyses were performed to characterize the EE of modern MAM technologies, particularly the systems presented in this paper. Despite MAM's high process energy impact compared to TM, some techniques have been shown to improve EE. Increasing machine utilization, for example, can have a considerable effect on reducing the SEC per part and is one of the most influential factors when it comes to EE. Moreover, printing several parts as opposed to one requires very little energy. [230]. Additionally, machines that print one part per week and are left idle between cycles can have 95 times the environmental impact of printers that run at maximum capacity. Likewise, increasing the number of parts per print can more widely distribute energy consumption for systems with high startup and cool-down loads [231].

The theoretical SEC of a MAM process can be calculated efficiently with only several pieces of information, providing the user has access to the system's integrated software, and the average daily energy consumption has been acquired. This can usually be found in the machine's documentation or by requesting data from the manufacturer. Once the average daily consumption ($E_{(kWh/day)}$) is known, the user can divide this by the number of hours per day ($T_{(h/day)}$) to obtain an hourly average shown in Eq. (1)

$$E_{(kWh)} = \frac{E_{(kWh/day)}}{T_{(h/day)}} \quad (1)$$

Once the average hourly energy consumption ($E_{(kWh)}$) has been established; a 3D CAD model can be designed with a mass of 1 kg. The file can then be uploaded to the machine, and a print time can be determined. ($P_{(h)}$) can then be multiplied by the hourly energy consumption to define the SEC shown in Eq. (2):

$$SEC = P_{(h)} \times E_{(kWh)} \quad (2)$$

The above method can achieve an accurate degree of certainty; however, validating the SEC by empirical energy monitoring is also worthwhile. The impact in terms of CO_2 equivalent per kg (CO_2eq/kg) can also be quantified by multiplying the SEC with the present carbon intensity conversion factor for a particular country or region. While

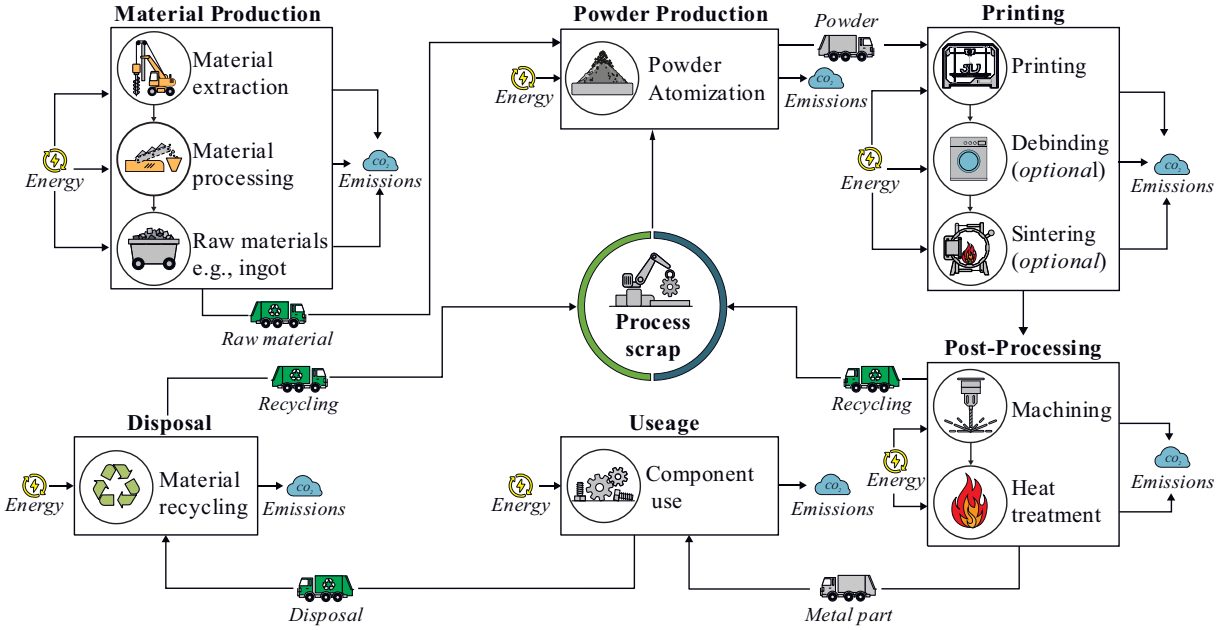

Fig. 10. Example of the typical phases included in the life cycle of a MAM product.

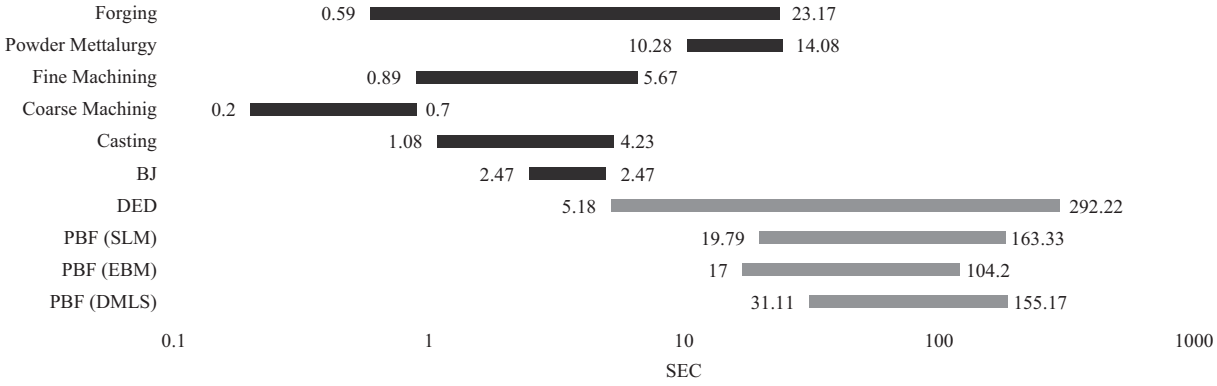

Fig. 11. SEC comparison of MAM and TM processes [229].

these metrics are two important indicators, they do not provide a complete representation of a product's sustainable credentials, which is why comprehensive LCA databases are needed to substantiate the total energy consumption and CO_2eq through cradle-to-grave LCAs [232]. Despite the relationship between some techniques to improve the EE of the printing phase, until reliable datasets have been created, it is unclear whether similar relationships exist among other stages in the lifecycle. However, once the work has been done, there is an opportunity for researchers and manufacturers to integrate energy metrics into future MAM technologies so users can appreciate the environmental impact of printing products. A predictive impact tool or a CAD-integrated software program based on accurate LCA data would be even more advantageous. This would allow users to determine, in advance, the difference between AM and TM processes and could also be used to understand the influence of optimizing designs and adjusting process parameters. Companies that use MAM may also benefit from tools and techniques used in other industries to improve EE. For instance, a small-scale study found that in some industries, energy management systems (EnMS) have been shown to improve EE by as much as 14 % [233]. An EnMS focuses on reducing resources and waste by optimizing systems and equipment through energy usage plans and measures by developing strategies that address a company's energy objectives and how and when they will be achieved by monitoring their EE progress.

Similarly, continuous energy auditing has also reduced barriers to EE in foundries by understanding the quality and quantity of how and where energy is being used [234] and is one of the most valuable sources of information for EE [235]. A lack of awareness of energy policies, poorly targeted incentives, lack of internal competence on energy management issues, and lack of project accountability have also been shown to be fundamental barriers to EE in some workplaces and implementing strategies that recognize issues relating to sustainability through targeted training programs; EE can be improved by up to 10 % [236]. This can be especially useful for machine operators to maximize utilization of the print bed and reduce idling times.

Overall, AM was never meant to replace TM as a more sustainable manufacturing process; instead, it was developed to create complex geometries that were nearly impossible to manufacture conventionally. Even though the existing literature indicates that MAM is typically less sustainable because of its high SEC, its characteristics mean it can be harnessed to reduce the environmental impact of products in some instances. Conversely, there are other times when AM is the less sustainable option, as is the case for mass production [221]. Nonetheless, many industries are benefiting from AM's ability to increase the longevity of products that are also more advanced, complex, and lighter. However,

until the work has been done to characterize the whole AM process, there is limited visibility or transparency on the environmental impact of MAM for users and consumers. Cooperation by stakeholders at all levels can help further the understanding of the potential ecological impacts of AM. In the meantime, best practices based on techniques shown to reduce energy consumption would be helpful. Therefore, the framework in Table 39 could be used as a basis to improve overall sustainability.

10. Conclusion

This article comprehensively reviewed four MAM technologies, namely ME, PBF, BJ, and DED, including their recent achievements. The main challenges and considerations of state of the art in terms of future development were outlined and discussed. However, it is important to note that other fundamental subjects such as process standardization, data acquisition, DfAM, novel materials, economics, ethical and social issues, and others are also significant to MAM's progress and have been intentionally omitted from this article and reserved more focused studies. Overall, this work provides a contemporary summary of some of the most relevant topics in this field of MAM and is intended to be particularly useful for practicing engineers, technologists, and researchers.

Modern MAM technology has become one of the most innovative technologies in the manufacturing industry. Compared to TM techniques, it can be used to fabricate complex and lightweight structures that would otherwise be too costly and time-consuming to manufacture. It also offers other advantages, such as the ability to consolidate large assemblies and create NNS components without expensive tooling, as well as the option of further enhancing its efficiency by applying DfAM methodologies such as topology and material optimization techniques. As an industry, it has evolved from prototyping to now producing advanced products as a result of advancements in hardware and software and metallurgy developments. The increased attention of the scientific community and the rate of growth in recent years also suggest that MAM could play an instrumental role in facilitating a transition to the next industrial revolution as well as providing industry with an alternative means of mass-producing metal products in the future. However, there are still some opportunities for improvement, including several technical challenges to overcome before this can be accomplished. For instance, even though all MAM processes have demonstrated their ability to produce parts with equivalent and sometimes superior mechanical properties to their wrought counterparts, there are many variables that can be adjusted during the printing process, each of which has a certain influence on the part's final characteristics. Because of this, it can be challenging to determine the optimal combination of parameters to improve one property without adversely affecting others, given the complex thermal processes involved in fusing metal particles together in a layer-by-layer fashion. As this is a manufacturing method unlike any other, optimizing the entire process to attain specific part characteristics can be a challanging undertaking to satisfy often competing design requirements.

Table 39
Recommendations for EE improvements for MAM.

EE procedure	Description
Printing at maximum capacity	Can help reduce energy consumption if the print bed utilization is maximized. Printers should also be switched off when not in use.
Topology optimization	Can help reduce the amount of material required for a part, thereby reducing print times and energy consumption.
Part consolidation	Consolidating an assembly to a minimum number of parts can reduce material use, print times, and assembly times, thereby reducing energy use and emissions.
Processing parameters	Can help mitigate increased printing times. The height of the part in the z-direction should be minimized (consider printing orientation), and parts should be designed to minimize support material.
Material optimization	Materials should be selected to fulfill the application's requirements based on the most sustainable option.
EnMs	Optimizing systems and equipment by implementing energy usage plans and measures can reduce resources and unnecessary waste.
Continuous energy auditing	Can help to understand the quality and quantity of materials and how and where energy is used.
Training and Awareness	Training staff to understand sustainability issues can encourage EE consumption and waste reduction, instate values and foster healthy working practices.

Although the scientific community has made significant strides toward understanding the effects of most of these important parameters in terms of their influence on surface characteristics, tolerances, and defects such as porosity formation, RS, microstructure, and others, the industry is still far from being able to print metallic parts with reliable and repeatable mechanical properties in the same way conventional methods can. While these centuries-old techniques, such as casting, forging, turning, and milling, have been perfected over time, it is important to remember that MAM is a relatively new technology, having only existed for approximately 40 years. As a result, a knowledge base of comparable magnitude has not yet been established. Nevertheless, failure to define these relationships will adversely affect MAM's ability to manufacture consistently high-quality products, making it economically and technically unviable as a method of mass-producing metallic parts.

While efforts continue to be made to improve the quality of printed products, some broader approaches would be helpful. An example would be the development of a concise guide or set of benchmarking policies based on the latest knowledge of the relationship between processing-structure-property relationships in order to assist users in selecting parameters that minimize the risk of common defects. In particular, those new to additive technologies would benefit from this interim approach.

For now, there is evidence that certain techniques can mitigate some of the shortcomings associated with MAM. One example is the work being undertaken to enhance the capabilities of in-situ and predictive monitoring of closed-loop autonomous control systems. Progress in this area would facilitate pattern recognition programs to detect common defects earlier in the process, resulting in a significant increase in productivity. However, many techniques developed so far only address monitoring processes rather than identifying correlations between process parameters and material discontinuities. While these technologies are still in the early stages of development, the present difficulty of large-scale data handling from multiple sensors to recognize patterns is possibly one of the most significant barriers to creating intelligent control systems. ML holds considerable promise in this area; however, the computational costs associated are presently too expensive. Another recent mitigation technique that has shown some practical benefit is the development of HAM which combines MAM and TM processes. These machines have shown promise by significantly reducing the number of metallurgical defects. As a consequence, these technologies can greatly diminish the need for labor-intensive and manual post-processing. There have already been several HAM machines developed, but much more work is still needed to fully understand their value and the implications of this technology for the industry. An example would be the effects of cutting fluids on the frequency of cracking. There are also other factors that merit further investigation, including HAM's longer processing times and its potential limitations concerning the processing of hard-to-machine alloys. However, the more significant issue is that few people currently possess the knowledge and expertise necessary to operate and program HAM machines.

While extensive research is being carried out on MAM processes, it may take decades before MAM becomes a reliable technique for producing large quantities of defect-free parts with predictable mechanical characteristics. While this milestone may well be many years away, there is no reason to discourage the scientific community or industry

from investing substantial resources in the development of MAM. After all, it took the internet more than 25 years to revolutionize commerce following its 1969 inception. Nor was everyone convinced that the internet would assume a central role in our lives—one newspaper editorial from the 1990s stated that "no online database will replace your daily newspaper, no CD-ROM can take the place of a competent teacher, and no computer network will change the way government works." Despite those expectations, the internet has revolutionized how the world works and communicates. This suggests that MAM may follow a similar trajectory in the future; however, such an achievement can only be reached by continuing, coordinated, and collaborative research efforts among stakeholders from various disciplines. In terms of the main challenges for MAM, the main conclusions from the literature can be summarized as follows:

ME

- ME is mainly characterized by the ADAM and BMD processes that use a filament to fabricate structures by extruding it through a nozzle. Despite their relative affordability and the ability to produce parts with high geometrical accuracy, these parts suffer from high porosity and poor surface finishes. As far as the characterization of the process-structure-property relationship is concerned, insufficient research has been conducted. Despite evidence suggesting that vertically oriented parts have lower mechanical properties than other orientations, there is conflicting information concerning the difference between either flat or on-edge parts. The impact of LT on mechanical properties is also unclear, and the representation of the influence of different infill strategies is also understudied. In addition, no other commercial material intended for these processes has been evaluated other than 17–4PH SS. It should also be noted that the environmental impact of ME has not been investigated either. As a result, there is still a considerable amount of uncertainty regarding the characteristics of ME, which offers the prospect of further research and development that may result in improvements to the process and quality of parts.

BJ

- The underlying mechanisms of BJ are multifaceted, involving numerous interactions between various substances. The optimum selection of process parameters and the powder characteristics are both crucial factors in printing defect-free metal parts. Although porosity continues to pose a significant challenge to the development of BJ, perhaps understanding and controlling shrinkage may be one of its most critical challenges. Shrinkage can be mitigated to a certain extent during the design stage. This, however, requires a high level of experience and is not always a reliable approach. A better way would be the development of integrated intelligent monitoring and control systems that can mitigate these incidents in situ. Despite an increased understanding of defect formation, a limited number of studies have been conducted to establish robust causal links between processing conditions and defect formation. Although efforts are being made to improve the process, only a few commercial materials are available, and their properties have not been adequately characterized. The impact of BJ on the environment has also received limited research attention.

PBF

- By using a thermal source to melt or sinter powder particles layer by layer, PBF is one of the most widely used technologies today for printing metallic parts. While it can process a wide range of materials, the complex melt pool mechanisms render it susceptible to several significant defects. These include high surface roughness, porosity, and RS. It is still unclear how most of these defects are related to the many variables involved in PBF, despite numerous attempts to describe and mitigate these through various strategies. HAM processes have shown a clear potential for improving the quality of PBF parts; however, sufficient research has not yet been conducted to define their exact implication. There is also considerable scope for integrating multiple process sensors to enable a more comprehensive understanding of the relationship of the process's many variables and part characteristics, in addition to developing ML algorithms for anomaly detection and closed-loop control. While these are all under investigation, developing novel process sensing approaches or strategies for sensor integration remains a significant area of opportunity for future research.

DED

- Due to a similar melting mechanism, DED typically suffers from many of the same limitations as PBF, including RS, porosity, high surface roughness as well as cracks, and delamination. Being notable for its RR capability and ability to fabricate relatively larger structures than other MAM technologies, DED also has the advantage of being able to process not only a wide variety of materials but also produce multi-material parts. Despite this, the influence of processing variables is still largely unknown. Further studies on establishing a correlation between these variables and the resultant part properties would be highly beneficial to the advancement of DED. Due to the significant number of resources dedicated to DED-HAM development, it is expected to improve the applicability of this technology significantly. Even though many hybrid systems are commercially available and their parts exhibit promising mechanical properties, they remain understudied, and their implications for the future remain unclear.

Sustainability

- It is important to note that the issue of sustainability remains largely unaddressed. A common perception is that MAM is more environmentally friendly than some TM methodologies. This notion is typically attributed to its ability to reduce waste and eliminate unnecessary steps in the manufacturing process. However, since the environmental assessment models developed to date are based solely on general life cycle assessments, the true environmental impact is unclear. These generic models may be helpful in the context of TM techniques. However, they are less relevant when it comes to MAM. This is because the databases for printed materials are not well developed. Additionally, MAM offers unique capabilities in terms of its design freedom, which is often overlooked. In and of itself, this may have a significant impact on sustainability. It is, therefore, necessary to develop specific datasets as well as frameworks that account for these nuanced aspects of MAM in order to be able to determine its true environmental impact. Despite this, the majority of current literature on this topic focuses exclusively on the SEC of the printing process. In this context, it is clear that MAM has a significantly more significant impact per kg than TM. However, several techniques have been identified that could enhance the EE of the process. Among the other points mentioned in this article, they include printing at maximum capacity, selecting structurally and environmentally sound materials, and implementing energy management systems.

Declaration of competing interest

The authors declare that they have no known competing financial interests or personal relationships that could have appeared to influence the work reported in this paper.

References

[1] Jamwal A, Agrawal R, Sharma M, Giallanza A. Industry 4.0 technologies for manufacturing sustainability: a systematic review and future research directions. Appl Sci 2021;11:5725. https://doi.org/10.3390/app11125725.

[2] Xu X, Lu Y, Vogel-Heuser B, Wang L. Industry 4.0 and industry 5.0—inception, conception and perception. J Manuf Syst 2021;61:530–5. https://doi.org/10.1016/j.jmsy.2021.10.006.

[3] Johnson NS, Vulimiri PS, To AC, Zhang X, Brice CA, Kappes BB, Stebner AP. Invited review: machine learning for materials developments in metals additive

manufacturing. Addit Manuf 2020;36:101641. https://doi.org/10.1016/j.addma.2020.101641.
[4] Gardan J. Additive manufacturing technologies: state of the art and trends. In: Addit. Manuf. Handb. Prod. Dev. Def. Ind. CRC Press; 2017. p. 149–68. https://doi.org/10.1201/9781315119106.
[5] Technical Committee AMT/8. In: BS EN ISO/ASTM 52900: additive manufacturing - general principles - terminology. Int. Stand.; 2017. p. 1–30.
[6] Tofail SAM, Koumoulos EP, Bandyopadhyay A, Bose S, O'Donoghue L, Charitidis C. Additive manufacturing: scientific and technological challenges, market uptake and opportunities. Mater Today 2018;21:22–37. https://doi.org/10.1016/j.mattod.2017.07.001.
[7] Jamróz W, Szafraniec J, Kurek M, Jachowicz R. 3D printing in pharmaceutical and medical applications – recent achievements and challenges. Pharm Res 2018;35:176. https://doi.org/10.1007/s11095-018-2454-x.
[8] Blakey-Milner B, Gradl P, Snedden G, Brooks M, Pitot J, Lopez E, Leary M, Berto F, du Plessis A. Metal additive manufacturing in aerospace: a review. Mater Des 2021;209:110008. https://doi.org/10.1016/j.matdes.2021.110008.
[9] Gradl PR, Teasley T, Protz C, Katsarelis C, Chen P. Process development and hot-fire testing of additively manufactured NASA HR-1 for liquid rocket engine applications. In: AIAA propuls. energy forum, 2021. American Institute of Aeronautics and Astronautics Inc, AIAA; 2021. https://doi.org/10.2514/6.2021-3236.
[10] Gardner L, Kyvelou P, Herbert G, Buchanan C. Testing and initial verification of the world's first metal 3D printed bridge. J Constr Steel Res 2020;172:106233. https://doi.org/10.1016/j.jcsr.2020.106233.
[11] Altıparmak SC, Xiao B. A market assessment of additive manufacturing potential for the aerospace industry. J Manuf Process 2021;68:728–38. https://doi.org/10.1016/j.jmapro.2021.05.072.
[12] Song B, Zhao X, Li S, Han C, Wei Q, Wen S, Liu J, Shi Y. Differences in microstructure and properties between selective laser melting and traditional manufacturing for fabrication of metal parts: a review. FrontMech. Eng. 2015;10:111–25. https://doi.org/10.1007/s11465-015-0341-2.
[13] Sanaei N, Fatemi A. Defects in additive manufactured metals and their effect on fatigue performance: a state-of-the-art review. Prog Mater Sci 2021;117:100724. https://doi.org/10.1016/j.pmatsci.2020.100724.
[14] Narasimharaju SR, Zeng W, See TL, Zhu Z, Scott P, Jiang X, Lou S. A comprehensive review on laser powder bed fusion of steels: processing, microstructure, defects and control methods, mechanical properties, current challenges and future trends. J Manuf Process 2022;75:375–414. https://doi.org/10.1016/j.jmapro.2021.12.033.
[15] Kok Y, Tan XP, Wang P, Nai MLS, Loh NH, Liu E, Tor SB. Anisotropy and heterogeneity of microstructure and mechanical properties in metal additive manufacturing: a critical review. Mater Des 2018;139:565–86. https://doi.org/10.1016/j.matdes.2017.11.021.
[16] Kurose T, Abe Y, Santos MVA, Kanaya Y, Ishigami A, Tanaka S, Ito H. Influence of the layer directions on the properties of 316l stainless steel parts fabricated through fused deposition of metals. Materials (Basel) 2020;13:2493. https://doi.org/10.3390/ma13112493.
[17] Suwanpreecha C, Manonukul A. On the build orientation effect in as-printed and as-sintered bending properties of 17–4PH alloy fabricated by metal fused filament fabrication. Rapid Prototyp J 2022;28:1076–85. https://doi.org/10.1108/RPJ-07-2021-0174.
[18] Wüst P, Edelmann A, Hellmann R. Areal surface roughness optimization of maraging steel parts produced by hybrid additive manufacturing. Materials (Basel) 2020;13. https://doi.org/10.3390/ma13020418.
[19] Guo C, Li S, Shi S, Li X, Hu X, Zhu Q, Ward RM. Effect of processing parameters on surface roughness, porosity and cracking of as-built IN738LC parts fabricated by laser powder bed fusion. J Mater Process Technol 2020;285:116788. https://doi.org/10.1016/j.jmatprotec.2020.116788.
[20] Henry TC, Morales MA, Cole DP, Shumeyko CM, Riddick JC. Mechanical behavior of 17–4 PH stainless steel processed by atomic diffusion additive manufacturing. Int J Adv Manuf Technol 2021. https://doi.org/10.1007/s00170-021-06785-1.
[21] Haghdadi N, Laleh M, Moyle M, Primig S. Additive manufacturing of steels: a review of achievements and challenges. J Mater Sci 2021;56:64–107. https://doi.org/10.1007/s10853-020-05109-0.
[22] Bandyopadhyay A, Zhang Y, Bose S. Recent developments in metal additive manufacturing. Curr Opin Chem Eng 2020;28:96–104. https://doi.org/10.1016/j.coche.2020.03.001.
[23] Dowling L, Kennedy J, O'Shaughnessy S, Trimble D. A review of critical repeatability and reproducibility issues in powder bed fusion. Mater Des 2020;186:108346. https://doi.org/10.1016/j.matdes.2019.108346.
[24] Joshi D, Ravi B. Quantifying the shape complexity of cast parts. Comput Aided Des Appl 2010;7:685–700. https://doi.org/10.3722/cadaps.2010.685-700.
[25] Hopkinson N, Hague RJM, Dickens PM. Rapid manufacturing: an industrial revolution for the Digital Age. 2006. https://doi.org/10.1002/0470033991.
[26] Pradel P, Zhu Z, Bibb R, Moultrie J. Complexity is not for free : the impact of component complexity on additive manufacturing build time. In: 15th Conf. Rapid Des. Prototyp. Manuf; 2017. p. 0–8.
[27] Jared BH, Boyce B, Battaille CC, Lim H, Tran HD, Robbins J, Clark BW, Blacker TD. Complexity isn't necessarily free: Opportunities and challenges in additive manufacturing. In: Proc. - ASPE 2015 Spring Top. Meet. Achiev. Precis. Toler. Addit. Manuf., United States. Washington, D.C.: National Nuclear Security Administration; 2015. p. 22–5.
[28] Thellaputta GR, Chandra PS, Rao CSP. Machinability of nickel based superalloys: a review. In: Mater. Today Proc. Elsevier Ltd; 2017. p. 3712–21. https://doi.org/10.1016/j.matpr.2017.02.266.
[29] Khanna N, Zadafiya K, Patel T, Kaynak Y, Rahman Rashid RA, Vafadar A. Review on machining of additively manufactured nickel and titanium alloys. J Mater Res Technol 2021;15:3192–221. https://doi.org/10.1016/j.jmrt.2021.09.088.
[30] Zhang C, Wang S, Li J, Zhu Y, Peng T, Yang H. Additive manufacturing of products with functional fluid channels: a review. Addit Manuf 2020;36:101490. https://doi.org/10.1016/j.addma.2020.101490.
[31] Prakash C, Singh S, Kopperi H, Ramakrihna S, Mohan SV. Comparative job production based life cycle assessment of conventional and additive manufacturing assisted investment casting of aluminium: a case study. Elsevier; 2021. https://doi.org/10.1016/j.jclepro.2020.125164.
[32] Khorasani M, Ghasemi AH, Rolfe B, Gibson I. Additive manufacturing a powerful tool for the aerospace industry. Rapid Prototyp J 2022;28:87–100. https://doi.org/10.1108/RPJ-01-2021-0009.
[33] Herzog D, Seyda V, Wycisk E, Emmelmann C. Additive manufacturing of metals. Acta Mater 2016;117:371–92. https://doi.org/10.1016/j.actamat.2016.07.019.
[34] Rouf S, Malik A, Singh N, Raina A, Naveed N, Siddiqui MIH, Haq MIU. Additive manufacturing technologies: industrial and medical applications. Sustain Oper Comput 2022;3:258–74. https://doi.org/10.1016/j.susoc.2022.05.001.
[35] Gibson I, Rosen D, Stucker B. Directed energy deposition processes. In: Addit. Manuf. Technol. New York: Springer; 2015. p. 245–68. https://doi.org/10.1007/978-1-4939-2113-3_10.
[36] Mostafaei A, Elliott AM, Barnes JE, Li F, Tan W, Cramer CL, Nandwana P, Chmielus M. Binder jet 3D printing—process parameters, materials, properties, modeling, and challenges. Prog. Mater. Sci. 2021;119:100707. https://doi.org/10.1016/j.pmatsci.2020.100707.
[37] Gibson I, Rosen D, Stucker B, Khorasani M. Binder jetting. In: Addit. Manuf. Technol. Cham: Springer; 2021. p. 237–52. https://doi.org/10.1007/978-3-030-56127-7_8.
[38] Gonzalez-Gutierrez J, Cano S, Schuschnigg S, Kukla C, Sapkota J, Holzer C. Additive manufacturing of metallic and ceramic components by the material extrusion of highly-filled polymers: a review and future perspectives. Materials (Basel) 2018;11:840. https://doi.org/10.3390/ma11050840.
[39] Frazier WE. Metal additive manufacturing: a review. J Mater Eng Perform 2014;23:1917–28. https://doi.org/10.1007/s11665-014-0958-z.
[40] Sames WJ, List FA, Pannala S, Dehoff RR, Babu SS. The metallurgy and processing science of metal additive manufacturing. Int Mater Rev 2016;61:315–60. https://doi.org/10.1080/09506608.2015.1116649.
[41] Zhang Y, Wu L, Guo X, Kane S, Deng Y, Jung YG, Lee JH, Zhang J. Additive manufacturing of metallic materials: a review. J Mater Eng Perform 2018;27:1–13. https://doi.org/10.1007/s11665-017-2747-y.
[42] Galati M, Minetola P. Analysis of density, roughness, and accuracy of the atomic diffusion additive manufacturing (ADAM) process for metal parts. Materials (Basel) 2019;12:4122. https://doi.org/10.3390/ma1224122.
[43] Waalkes L, Längerich J, Holbe F, Emmelmann C. Feasibility study on piston-based feedstock fabrication with Ti-6Al-4V metal injection molding feedstock. Addit Manuf 2020;35:101207. https://doi.org/10.1016/j.addma.2020.101207.
[44] Watson A, Belding J, Ellis BD. Characterization of 17-4 PH processed via bound metal deposition (BMD). In: Miner. Met. Mater. Ser. Springer; 2020. p. 205–16. https://doi.org/10.1007/978-3-030-36296-6_19.
[45] Du W, Singh M, Singh D. Binder jetting additive manufacturing of silicon carbide ceramics: development of bimodal powder feedstocks by modeling and experimental methods. Ceram Int 2020;46:19701–7. https://doi.org/10.1016/j.ceramint.2020.04.098.
[46] Desktop Metal Inc., Shop System, (n.d.). https://www.desktopmetal.com/products/shop (accessed May 7, 2021).
[47] Production system. https://www.desktopmetal.com/products/production; 2020 (accessed April 23, 2021).
[48] Spee3D, LightSPEE3D 3D Metal Printer, (n.d.). https://spee3d.com/product/lightspee3d/ (accessed April 23, 2021).
[49] Scime L, Haley J, Paquit V. Monitoring for additive manufacturing technologies: report on progress, achievements, and limitations of monitoring techniques, Oak Ridge, TN (United States). 2019. https://doi.org/10.2172/1823379.
[50] Gallant LG, Hsiao A, McSorley G. Benchmark physical and mechanical property chararacterization of 316L stainless steel dmls prints. In: Prog. Can. Mech. Eng. 4. Robertson Library, Charlottetown, P.E.I.: University of Prince Edward Island; 2021. https://doi.org/10.32393/csme.2021.217.
[51] Khorasani AM, Gibson I, Veetil JK, Ghasemi AH. A review of technological improvements in laser-based powder bed fusion of metal printers. Int J Adv Manuf Technol 2020;108:191–209. https://doi.org/10.1007/s00170-020-05361-3.
[52] Additec, M450, (n.d.). https://www.additec.net/m450 (accessed April 23, 2021).
[53] Piscopo G, Iuliano L. Current research and industrial application of laser powder directed energy deposition. Int J Adv Manuf Technol 2022:1–25. https://doi.org/10.1007/s00170-021-08596-w.
[54] Tepylo N, Huang X, Patnaik PC. Laser-based additive manufacturing technologies for aerospace applications. Adv Eng Mater 2019;21. https://doi.org/10.1002/adem.201900617.
[55] Vafadar A, Guzzomi F, Rassau A, Hayward K. Advances in metal additive manufacturing: a review of common processes, industrial applications, and current challenges. Appl Sci 2021;11:1–33. https://doi.org/10.3390/app11031213.
[56] Bouaziz MA, Djouda JM, Kauffmann J, Hild F. Microscale mechanical characterization of 17-4PH stainless steel fabricated by atomic diffusion additive manufacturing (ADAM). In: Procedia Struct. Integr. Elsevier B.V.; 2020. p. 1039–46. https://doi.org/10.1016/j.prostr.2020.11.119.

[57] Crump SS. United States Patent - US5121329A - apparatus and method for creating three-dimensional objects. 1989.
[58] Carroll BE, Palmer TA, Beese AM. Anisotropic tensile behavior of ti-6Al-4V components fabricated with directed energy deposition additive manufacturing. Acta Mater 2015;87:309–20. https://doi.org/10.1016/j.actamat.2014.12.054.
[59] Unger L, Scheideler M, Meyer P, Harland J, Görzen A, Wortmann M, Dreyer A, Ehrmann A. Increasing adhesion of 3D printing on textile fabrics by polymer coating. Tekstilec 2018;61:265–71. https://doi.org/10.14502/Tekstilec2018.61.265-271.
[60] Nurhudan AI, Supriadi S, Whulanza Y, Saragih AS. Additive manufacturing of metallic based on extrusion process: a review. J Manuf Process 2021;66:228–37. https://doi.org/10.1016/j.jmapro.2021.04.018.
[61] Banerjee S, Joens CJ. Debinding and sintering of metal injection molding (MIM) components. In: Handb. Met. Inject. Molding. Elsevier Inc.; 2012. p. 133–80. https://doi.org/10.1533/9780857096234.1.133.
[62] Campbell IW, Wohlers T. Markforged: taking a different approach to metal additive manufacturing. Met AM 2017;3:113–6.
[63] Metal Desktop, et al. In: Studio system furnace specifications; 2019. p. 2 (accessed April 24, 2021), https://www.desktopmetal.com/products/studio.
[64] Granta Design Limited. Granta EduPack sotfware. Granta Des; 2020.
[65] Markforged Inc. H13 tool steel - material datasheet. 2018 (accessed April 26, 2021), https://static.markforged.com/downloads/h13-tool-steel.pdf.
[66] H13 tool steel - material datasheet; 2021. p. 1 (accessed April 24, 2021), https://www.desktopmetal.com/uploads/DM-0015-00-Studio_MDS_H13-v1.3.pdf.
[67] Markforged Inc. In: Copper - material datasheet; 2020. p. 1 (accessed April 26, 2021), http://static.markforged.com/downloads/copper-data-sheet.pdf.
[68] Markforged Inc. In: Desktop Metal Inc., copper - material datasheet; 2020. p. 1 (accessed April 26, 2021), http://static.markforged.com/downloads/copper-data-sheet.pdf.
[69] Rane K, Strano M. A comprehensive review of extrusion-based additive manufacturing processes for rapid production of metallic and ceramic parts. Adv Manuf 2019;7:155–73. https://doi.org/10.1007/s40436-019-00253-6.
[70] Tosto C, Tirillò J, Sarasini F, Cicala G. Hybrid metal/polymer filaments for fused filament fabrication (FFF) to print metal parts. Appl Sci 2021;11:1. https://doi.org/10.3390/app11041444.
[71] Suwanpreecha C, Seensattayawong P, Vadhanakovint V, Manonukul A. Influence of specimen layout on 17–4PH (AISI 630) alloys fabricated by low-cost additive manufacturing. Metall Mater Trans A Phys Metall Mater Sci 2021;52:1999–2009. https://doi.org/10.1007/s11661-021-06211-x.
[72] Caminero MÁ, Romero A, Chacón JM, Núñez PJ, García-Plaza E, Rodríguez GP. Additive manufacturing of 316L stainless-steel structures using fused filament fabrication technology: mechanical and geometric properties. Rapid Prototyp J 2021;27:583–91. https://doi.org/10.1108/RPJ-06-2020-0120.
[73] Godec D, Cano S, Holzer C, Gonzalez-Gutierrez J. Optimization of the 3D printing parameters for tensile properties of specimens produced by fused filament fabrication of 17–4PH stainless steel. Materials (Basel) 2020;13:774. https://doi.org/10.3390/ma13030774.
[74] Singh P, Balla VK, Atre SV, German RM, Kate KH. Factors affecting properties of ti-6Al-4V alloy additive manufactured by metal fused filament fabrication. Powder Technol 2021;386:9–19. https://doi.org/10.1016/j.powtec.2021.03.026.
[75] Campbell Q, Filiault M, Rooney K, Belding J, Ellis BD. In: TechConnect Briefs; 2019. p. 139–42.
[76] Ziaee M, Crane NB. Binder jetting: a review of process, materials, and methods. Addit Manuf 2019;28:781–801. https://doi.org/10.1016/j.addma.2019.05.031.
[77] Mirzababaei S, Pasebani S. A review on binder jet additive manufacturing of 316L stainless steel. J Manuf Mater Process 2019;3:82. https://doi.org/10.3390/jmmp3030082.
[78] Atapour M, Wang X, Persson M, Odnevall Wallinder I, Hedberg YS. Corrosion of binder jetting additively manufactured 316L stainless steel of different surface finish. J Electrochem Soc 2020;167:131503. https://doi.org/10.1149/1945-7111/abb6cd.
[79] Miyanaji H, Zhang S, Yang L. A new physics-based model for equilibrium saturation determination in binder jetting additive manufacturing process. Int J Mach Tool Manuf 2018;124:1–11. https://doi.org/10.1016/j.ijmachtools.2017.09.001.
[80] Miyanaji H, Yang L. Equilibrium saturation in binder jetting additive manufacturing processes: theoretical model vs experimental observations. In: Solid Free. Fabr. 2016 Proc. 27th Annu. Int. Solid Free. Fabr. Symp. - An Addit. Manuf. Conf. SFF 2016; 2016. p. 1945–59.
[81] Lores A, Azurmendi N, Agote I, Zuza E. A review on recent developments in binder jetting metal additive manufacturing: materials and process characteristics. Powder Metall 2019;62:267–96. https://doi.org/10.1080/00325899.2019.1669299.
[82] Yegyan Kumar A, Bai Y, Eklund A, Williams CB. The effects of hot isostatic pressing on parts fabricated by binder jetting additive manufacturing. Addit Manuf 2018;24:115–24. https://doi.org/10.1016/j.addma.2018.09.021.
[83] Gibson I, Rosen DW, Stucker B. Additive manufacturing technologies: rapid prototyping to direct digital manufacturing. US: Springer; 2010. https://doi.org/10.1007/978-1-4419-1120-9.
[84] Rockland JGR. The determination of the mechanism of sintering. Acta Metall 1967;15:277–86. https://doi.org/10.1016/0001-6160(67)90203-9.
[85] German RM. Thermodynamics of sintering. In: Sinter. Adv. Mater. Elsevier; 2010. p. 3–32. https://doi.org/10.1533/9781845699949.1.3.
[86] Markforged Inc. Desktop Metal Inc., 3D printing materials. https://www.desktopmetal.com/materials; 2020 (accessed April 26, 2021).
[87] ExOne. ExOne metal 3D printing materials and binders. https://www.exone.com/en-US/3d-printing-materials-and-binders/metal-materials-binders; 2021 (accessed May 9, 2021).
[88] ExOne, 17-4PH Stainless Steel, (n.d.) 1. https://www.exone.com/Admin/getmedia/1e54b4df-198f-460e-95ff-bbf80d1d43b5/PSC_X1_MaterialData_17-4_SS_US_10192020_V6.pdf (accessed May 9, 2021).
[89] Huber D, Vogel L, Fischer A. The effects of sintering temperature and hold time on densification, mechanical properties and microstructural characteristics of binder jet 3D printed 17–4 PH stainless steel. Addit Manuf 2021;46:102114. https://doi.org/10.1016/j.addma.2021.102114.
[90] 17-4 PH stainless steel - shop system; 2020. p. 1 (accessed May 9, 2021), https://www.desktopmetal.com/uploads/SHP-SPC-MDS_17-4PH-210323.pdf.
[91] 17-4 PH stainless steel - production system; 2020. p. 1 (accessed May 9, 2021), https://www.desktopmetal.com/uploads/SPJ-SPC-MDS_17-4PH-210401-1.pdf.
[92] Hamidi MFFA, Harun WSW, Khalil NZ, Samykano M. Microstructural comparison and mechanical properties of stainless steel 316L fabricated by selective laser melting and metal injection moulding processes. Int J Manuf Technol Manag 2019;33:76–87. https://doi.org/10.1504/IJMTM.2019.100160.
[93] ExOne, 316L Stainless Steel, (n.d.). https://www.exone.com/Admin/getmedia/92ff696e-1b4e-4c7e-a45c-ae45b04340da/PSC_X1_MaterialData_316L_10192020_V6.pdf (accessed May 9, 2021).
[94] Lecis N, Mariani M, Beltrami R, Emanuelli L, Casati R, Vedani M, Molinari A. Effects of process parameters, debinding and sintering on the microstructure of 316L stainless steel produced by binder jetting. Mater Sci Eng A 2021;828. https://doi.org/10.1016/j.msea.2021.142108.
[95] Nastac M, Klein RLA. Microstructure and mechanical properties comparison of 316L parts produced by different additive manufacturing processes. In: Solid Free. Fabr. 2017 Proc. 28th Annu. Int. Solid Free. Fabr. Symp. - An Addit. Manuf. Conf. SFF 2017; 2020. p. 332–41.
[96] Inc Desktop Metal, et al. 316L stainless steel - production system. https://www.desktopmetal.com/uploads/SPJ-SPC-MDS_316L-210420.pdf; 2020.
[97] Nezhadfar PD, Verquin B, Lefebvre LP, Reynaud C, Robert M, Shamsaei N. Effect of heat treatment on the tensile behavior of 17-4 PH stainless steel additively manufactured by metal binder jetting, solid free. In: Fabr. 2019 Proc. 30th Annu. Int. Solid Free. Fabr. Symp. - An Addit. Manuf. Conf. SFF 2019; 2019. p. 2271–81. https://doi.org/10.26153/tsw/17611.
[98] Li M, Du W, Elwany A, Pei Z, Ma C. Metal binder jetting additive manufacturing: a literature review. J Manuf Sci Eng 2020;142. https://doi.org/10.1115/1.4047430.
[99] Ziaee M, Tridas EM, Crane NB. Binder-jet printing of fine stainless steel powder with varied final density. JOM 2017;69:592–6. https://doi.org/10.1007/s11837-016-2177-6.
[100] Chowdhury S, Anand S. Artificial neural network based geometric compensation for thermal deformation in additive manufacturing processes. American Society of Mechanical Engineers Digital Collection; 2016. https://doi.org/10.1115/msec2016-8784.
[101] Zago M, Lecis NFM, Vedani M, Cristofolini I. Dimensional and geometrical precision of parts produced by binder jetting process as affected by the anisotropic shrinkage on sintering. Addit Manuf 2021;43:102007. https://doi.org/10.1016/j.addma.2021.102007.
[102] Dini F, Ghaffari SA, Jafar J, Hamidreza R, Marjan S. A review of binder jet process parameters; powder, binder, printing and sintering condition. Met Powder Rep 2020;75:95–100. https://doi.org/10.1016/j.mprp.2019.05.001.
[103] Mao Y, Li J, Li W, Cai D, Wei Q. Binder jetting additive manufacturing of 316L stainless-steel green parts with high strength and low binder content: binder preparation and process optimization. J Mater Process Technol 2021;291:117020. https://doi.org/10.1016/j.jmatprotec.2020.117020.
[104] Hitzler L, Hirsch J, Heine B, Merkel M, Hall W, Öchsner A. On the anisotropic mechanical properties of selective laser-melted stainless steel. Materials (Basel) 2017;10. https://doi.org/10.3390/ma10101136.
[105] Doubenskaia MA, Zhirnov IV, Teleshevskiy VI, Bertrand P, Smurov IY. Determination of true temperature in selective laser melting of metal powder using infrared camera. Mater Sci Forum 2015;834:93–102. https://doi.org/10.4028/www.scientific.net/MSF.834.93.
[106] Kimura T, Nakamoto T. Microstructures and mechanical properties of A356 (AlSi7Mg0.3) aluminum alloy fabricated by selective laser melting. Mater Des 2016;89:1294–301. https://doi.org/10.1016/j.matdes.2015.10.065.
[107] van Zyl I, Yadroitsava I, Yadroitsev I. Residual stress in TI6AL4V objects produced by direct metal laser sintering, South African. J Ind Eng 2016;27:134–41. https://doi.org/10.7166/27-4-1468.
[108] Vock S, Klöden B, Kirchner A, Weißgärber T, Kieback B. Powders for powder bed fusion: a review. Prog Addit Manuf 2019;4:383–97. https://doi.org/10.1007/s40964-019-00078-6.
[109] Raza A, Fiegl T, Hanif I, MarkstrÖm A, Franke M, Körner C, Hryha E. Degradation of AlSi10Mg powder during laser based powder bed fusion processing. Mater Des 2021;198. https://doi.org/10.1016/j.matdes.2020.109358.
[110] Cheng Kong D, Fang Dong C, Qing Ni X, Zhang L, Xue Li R, He X, Man C, Gang Li X. Microstructure and mechanical properties of nickel-based superalloy fabricated by laser powder-bed fusion using recycled powders. Int J Miner Metall Mater 2021;28:266–78. https://doi.org/10.1007/s12613-020-2147-4.
[111] General Electric (GE) , Concept Laser M2 Series 5, (n.d.). https://www.ge.com/additive/additive-manufacturing/machines/m2series5 (accessed May 19, 2021).
[112] EOS GmbH. Electro optical systems, metal 3D printing materials and DMLS materials. https://www.eos.info/en/additive-manufacturing/3d-printing-metal/dmls-metal-materials; 2021.

[113] General Electric (GE). In: M2 Series 5 Steel 17-4 PH; 2021. p. 1–6 (accessed May 19, 2021), https://www.ge.com/additive/additive-manufacturing/machines/m2series5.
[114] Nezhadfar PD, Shrestha R, Phan N, Shamsaei N. Fatigue behavior of additively manufactured 17–4 PH stainless steel: synergistic effects of surface roughness and heat treatment. Int J Fatigue 2019;124:188–204. https://doi.org/10.1016/j.ijfatigue.2019.02.039.
[115] General Electric (GE). In: M2 Series 5 316L Stainless Steel Datasheet; 2021. p. 1–5 (accessed May 20, 2021), https://www.ge.com/additive/additive-manufacturing/machines/m2series5.
[116] Byun TS, Garrison BE, McAlister MR, Chen X, Gussev MN, Lach TG, Le Coq A, Linton K, Joslin CB, Carver JK, List FA, Dehoff RR, Terrani KA. Mechanical behavior of additively manufactured and wrought 316L stainless steels before and after neutron irradiation. J Nucl Mater 2021;548:152849. https://doi.org/10.1016/j.jnucmat.2021.152849.
[117] EOS, EOS StainlessSteel 316L. https://www.eos.info/03_system-related-assets/material-related-contents/metal-materials-and-examples/metal-material-datasheet/stainlesssteel/material_datasheet_eos_stainlesssteel_316l_en_web.pdf; 2020.
[118] Riikonen N, Piili H. Characterization of part deformations in laser powder bed fusion of stainless steel 316L. In: Procedia CIRP. Elsevier; 2020. p. 161–6. https://doi.org/10.1016/j.procir.2020.09.031.
[119] Kong D, Dong C, Ni X, Zhang L, Yao J, Man C, Cheng X, Xiao K, Li X. Mechanical properties and corrosion behavior of selective laser melted 316L stainless steel after different heat treatment processes. J Mater Sci Technol 2019;35:1499–507. https://doi.org/10.1016/j.jmst.2019.03.003.
[120] Ni M, Chen C, Wang X, Wang P, Li R, Zhang X, Zhou K. Anisotropic tensile behavior of in situ precipitation strengthened Inconel 718 fabricated by additive manufacturing. Mater Sci Eng A 2017;701:344–51. https://doi.org/10.1016/j.msea.2017.06.098.
[121] General Electric (GE), M2 series 5, n.d. https://www.ge.com/additive/additive-manufacturing/machines/m2series5 (accessed April 23, 2021).
[122] Witkin DB, Patel D, Albright TV, Bean GE, McLouth T. Influence of surface conditions and specimen orientation on high cycle fatigue properties of Inconel 718 prepared by laser powder bed fusion. Int J Fatigue 2020;132:105392. https://doi.org/10.1016/j.ijfatigue.2019.105392.
[123] Bean GE, McLouth TD, Witkin DB, Sitzman SD, Adams PM, Zaldivar RJ. Build orientation effects on texture and mechanical properties of selective laser melting inconel 718. J Mater Eng Perform 2019;28:1942–9. https://doi.org/10.1007/s11665-019-03980-w.
[124] GmbH E. Electro optical systems, EOS GmbH - electro optical systems, NickelAlloy IN718 material data sheet. https://www.eos.info/03_system-related-assets/material-related-contents/metal-materials-and-examples/metal-material-datasheet/nickelalloy-inconel/material_datasheet_eos_nickelalloy_in718_m290_premium_en_web.pdf; 2020.
[125] Daňa M, Zetková I, Mach J. Mechanical properties of Inconel alloy 718 produced by 3D printing using DMLS. Manuf Technol 2018;18:559–62. https://doi.org/10.21062/ujep/152.2018/a/1213-2489/MT/18/4/559.
[126] General Electric (GE). In: Material Datsheet AlSi10Mg, M2 Series 5; 2021. p. 2–5 (accessed December 18, 2021), https://www.ge.com/additive/additive-manufacturing/machines/m2series5.
[127] EOS GmbH. EOS aluminium AlSi10Mg material data sheet. https://www.eos.info/03_system-related-assets/material-related-contents/metal-materials-and-examples/metal-material-datasheet/aluminium/material_datasheet_eos_aluminium-alsi10mg_en_web.pdf; 2021 (accessed December 18, 2021).
[128] Zhang XX, Lutz A, Andrä H, Lahres M, Gan WM, Maawad E, Emmelmann C. Evolution of microscopic strains, stresses, and dislocation density during in-situ tensile loading of additively manufactured AlSi10Mg alloy. Int J Plast 2021;139:102946. https://doi.org/10.1016/j.ijplas.2021.102946.
[129] Girelli L, Tocci M, Gelfi M, Pola A. Study of heat treatment parameters for additively manufactured AlSi10Mg in comparison with corresponding cast alloy. Mater Sci Eng A 2019;739:317–28. https://doi.org/10.1016/j.msea.2018.10.026.
[130] Baxter CK, Cyr ED, Odeshi A, Mohammadi M. Mechanical behaviour and constitutive modeling of AlSi10Mg g-200°Cadditively manufactured through direct metal laser sintering. In: Proc. 16th Int. Alum. Alloy. Conf; 2018. p. 9.
[131] EOS. In: EOS M 290; 2019. p. 1–2 (accessed May 19, 2021), https://www.eos.info/en/additive-manufacturing/3d-printing-metal/eos-metal-systems/eos-m-290.
[132] Wang Q, Kong J, Liu X, Dong K, Song X, Yang Y, Xu J, Chen X. The effect of a novel low-temperature vacuum heat treatment on the microstructure and properties of Ti–6Al–4V alloys manufactured by selective laser melting. Vacuum 2021;193:110554. https://doi.org/10.1016/j.vacuum.2021.110554.
[133] Ju J, Li J, Yang C, Wang K, Kang M, Wang J. Evolution of the microstructure and optimization of the tensile properties of the Ti–6Al–4V alloy by selective laser melting and heat treatment. Mater Sci Eng A 2021;802:140673. https://doi.org/10.1016/j.msea.2020.140673.
[134] Marrey M, Malekipour E, El-Mounayri H, Faierson EJ. A framework for optimizing process parameters in powder bed fusion (PBF) process using artificial neural network (ANN). In: Procedia manuf. Elsevier B.V.; 2019. p. 505–15. https://doi.org/10.1016/j.promfg.2019.06.214.
[135] Ye C, Zhang C, Zhao J, Dong Y. Effects of post-processing on the surface finish, porosity, residual stresses, and fatigue performance of additive manufactured metals: a review. J Mater Eng Perform 2021;30:6407–25. https://doi.org/10.1007/s11665-021-06021-7.
[136] Vayssette B, Saintier N, Brugger C, El May M, Pessard E. Numerical modelling of surface roughness effect on the fatigue behavior of ti-6Al-4V obtained by additive manufacturing. Int J Fatigue 2019;123:180–95. https://doi.org/10.1016/J.IJFATIGUE.2019.02.014.
[137] Tian Y, Tomus D, Rometsch P, Wu X. Influences of processing parameters on surface roughness of hastelloy X produced by selective laser melting. Addit Manuf 2017;13:103–12. https://doi.org/10.1016/j.addma.2016.10.010.
[138] Rott S, Ladewig A, Friedberger K, Casper J, Full M, Schleifenbaum JH. Surface roughness in laser powder bed fusion – interdependency of surface orientation and laser incidence. Addit Manuf 2020;36:101437. https://doi.org/10.1016/j.addma.2020.101437.
[139] Feng S, Kamat AM, Sabooni S, Pei Y. Experimental and numerical investigation of the origin of surface roughness in laser powder bed fused overhang regions. Virtual Phys Prototyp 2021;16:S66–84. https://doi.org/10.1080/17452759.2021.1896970.
[140] Wang W, Garmestani H, Liang SY. Prediction of upper surface roughness in laser powder bed fusion. Metals (Basel) 2022;12:11. https://doi.org/10.3390/met12010011.
[141] Oliveira JP, LaLonde AD, Ma J. Processing parameters in laser powder bed fusion metal additive manufacturing. Mater Des 2020;193:108762. https://doi.org/10.1016/j.matdes.2020.108762.
[142] Promoppatum P, Srinivasan R, Quek SS, Msolli S, Shukla S, Johan NS, van der Veen S, Jhon MH. Quantification and prediction of lack-of-fusion porosity in the high porosity regime during laser powder bed fusion of ti-6Al-4V. J Mater Process Technol 2022;300:117426. https://doi.org/10.1016/j.jmatprotec.2021.117426.
[143] Al-Maharma AY, Patil SP, Markert B. Effects of porosity on the mechanical properties of additively manufactured components: a critical review. Mater Res Express 2020;7:122001. https://doi.org/10.1088/2053-1591/abcc5d.
[144] Malekipour E, El-Mounayri H. Common defects and contributing parameters in powder bed fusion AM process and their classification for online monitoring and control: a review. Int J Adv Manuf Technol 2018;95:527–50. https://doi.org/10.1007/s00170-017-1172-6.
[145] Montalbano T, Briggs BN, Waterman JL, Nimer S, Peitsch C, Sopcisak J, Trigg D, Storck S. Uncovering the coupled impact of defect morphology and microstructure on the tensile behavior of ti-6Al-4V fabricated via laser powder bed fusion. J Mater Process Technol 2021;294:117113. https://doi.org/10.1016/j.jmatprotec.2021.117113.
[146] Mirkoohi E, Liang SY, Tran HC, Lo YL, Chang YC, Lin HY. Mechanics modeling of residual stress considering effect of preheating in laser powder bed fusion. J Manuf Mater Process 2021;5:46. https://doi.org/10.3390/jmmp5020046.
[147] Bartlett JL, Li X. An overview of residual stresses in metal powder bed fusion. Addit Manuf 2019;27:131–49. https://doi.org/10.1016/j.addma.2019.02.020.
[148] Acevedo R, Sedlak P, Kolman R, Fredel M. Residual stress analysis of additive manufacturing of metallic parts using ultrasonic waves: state of the art review. J Mater Res Technol 2020;9:9457–77. https://doi.org/10.1016/j.jmrt.2020.05.092.
[149] Lu X, Cervera M, Chiumenti M, Lin X. Residual stresses control in additive manufacturing. J Manuf Mater Process 2021;5:138. https://doi.org/10.3390/jmmp5040138.
[150] McCann R, Obeidi MA, Hughes C, McCarthy É, Egan DS, Vijayaraghavan RK, Joshi AM, Acinas Garzon V, Dowling DP, McNally PJ, Brabazon D. In-situ sensing, process monitoring and machine control in laser powder bed fusion: a review. Addit Manuf 2021;45:102058. https://doi.org/10.1016/j.addma.2021.102058.
[151] Colosimo BM, Grasso M. In-situ monitoring in L-PBF: Opportunities and challenges. In: Procedia CIRP. Elsevier; 2020. p. 388–91. https://doi.org/10.1016/j.procir.2020.09.151.
[152] Moshiri M, Charles A, Elkaseer A, Scholz S, Mohanty S, Tosello G. An industry 4.0 framework for tooling production using metal additive manufacturing-based first-time-right smart manufacturing system. In: Procedia CIRP. Elsevier; 2020. p. 32–7. https://doi.org/10.1016/j.procir.2020.04.151.
[153] Grasso M, Remani A, Dickins A, Colosimo BM, Leach RK. In-situ measurement and monitoring methods for metal powder bed fusion: an updated review. Meas Sci Technol 2021;32. https://doi.org/10.1088/1361-6501/ac0b6b.
[154] Peng X, Kong L, An H, Dong G. A review of in situ defect detection and monitoring technologies in selective laser melting, 3D print. Addit Manuf 2022. https://doi.org/10.1089/3dp.2021.0114.
[155] Mahmoud D, Magolon M, Boer J, Elbestawi M, Mohammadi MG. Applications of machine learning in process monitoring and controls of L-PBF additive manufacturing: a review. Appl. Sci. 2021;11:11910. https://doi.org/10.3390/app112411910.
[156] Razvi SS, Feng S, Narayanan A, Lee YTT, Witherell P. A review of machine learning applications in additive manufacturing. In: Proc. ASME Des. Eng. Tech. Conf., American Society of Mechanical Engineers (ASME); 2019. https://doi.org/10.1115/DETC2019-98415.
[157] Meng L, McWilliams B, Jarosinski W, Park HY, Jung YG, Lee J, Zhang J. Machine learning in additive manufacturing: a review. JOM 2020;72:2363–77. https://doi.org/10.1007/s11837-020-04155-y.
[158] Sing SL, Kuo CN, Shih CT, Ho CC, Chua CK. Perspectives of using machine learning in laser powder bed fusion for metal additive manufacturing. Virtual Phys. Prototyp. 2021;16:372–86. https://doi.org/10.1080/17452759.2021.1944229.
[159] Goh GD, Sing SL, Yeong WY. A review on machine learning in 3D printing: applications, potential, and challenges. Artif Intell Rev 2021;54:63–94. https://doi.org/10.1007/s10462-020-09876-9.
[160] Pragana JPM, Sampaio RFV, Bragança IMF, Silva CMA, Martins PAF. Hybrid metal additive manufacturing: a state–of–the-art review. Adv. Ind. Manuf. Eng. 2021;2:100032. https://doi.org/10.1016/j.aime.2021.100032.
[161] Matsuura, LUMEX Avance-25, (n.d.). https://www.lumex-matsuura.com/english/lumex-avance-25 (accessed January 22, 2022).

[162] Matsuura, LUMEX Avance-60, (n.d.). https://www.lumex-matsuura.com/english/lumex-avance-60 (accessed January 22, 2022).
[163] S.E. Ltd., OPM250L, (n.d.). https://www.sodick.org/products/additive-manufacturing/opm250l.html (accessed January 22, 2022).
[164] S.E. Ltd., OPM350L, (n.d.). https://www.sodick.org/products/additive-manufacturing/opm350l.html (accessed January 22, 2022).
[165] G.H. 3D T. Co, HBD Metal 3D Printer, (n.d.). https://en.hb3dp.com/product/24.html (accessed January 22, 2022).
[166] A. Industries, MetalFABG2 Continuous Production, (n.d.). https://www.additiveindustries.com/metalfabg2-continuous-production (accessed January 22, 2022).
[167] Liu C, Yan D, Tan J, Mai Z, Cai Z, Dai Y, Jiang M, Wang P, Liu Z, Li CC, Lao C, Chen Z. Development and experimental validation of a hybrid selective laser melting and CNC milling system. Addit Manuf 2020;36:101550. https://doi.org/10.1016/j.addma.2020.101550.
[168] Mutua J, Nakata S, Onda T, Chen ZC. Optimization of selective laser melting parameters and influence of post heat treatment on microstructure and mechanical properties of maraging steel. Mater. Des. 2018;139:486–97. https://doi.org/10.1016/j.matdes.2017.11.042.
[169] Sarafan S, Wanjara P, Gholipour J, Bernier F, Osman M, Sikan F, Molavi-Zarandi M, Soost J, Brochu M. Evaluation of maraging steel produced using hybrid additive/subtractive manufacturing. J. Manuf. Mater. Process. 2021;5:107. https://doi.org/10.3390/jmmp5040107.
[170] Shen LC, Yang XH, Ho JR, Tung PC, Lin CK. Effects of build direction on the mechanical properties of a martensitic stainless steel fabricated by selective laser melting. Materials (Basel) 2020;13:1–18. https://doi.org/10.3390/ma13225142.
[171] Jiménez A, Bidare P, Hassanin H, Tarlochan F, Dimov S, Essa K. Powder-based laser hybrid additive manufacturing of metals: a review. Int J Adv Manuf Technol 2021;114:63–96. https://doi.org/10.1007/s00170-021-06855-4.
[172] Dilberoglu UM, Gharehpapagh B, Yaman U, Dolen M. Current trends and research opportunities in hybrid additive manufacturing. Int J Adv Manuf Technol 2021;113:623–48. https://doi.org/10.1007/s00170-021-06688-1.
[173] Yin Y, Tan Q, Bermingham M, Mo N, Zhang J, Zhang MX. Laser additive manufacturing of steels. Int. Mater. Rev. 2021. https://doi.org/10.1080/09506608.2021.1983351.
[174] Dutta B. Directed energy deposition (DED) technology. In: Ref. Modul. Mater. Sci. Mater. Eng. Elsevier; 2020. https://doi.org/10.1016/b978-0-12-819726-4.00035-1.
[175] Xu J, Lin X, Zhao Y, Guo P, Wen X, Li Q, Yang H, Dong H, Xue L, Huang W. HAZ liquation cracking mechanism of IN-738LC superalloy prepared by laser solid forming. Metall Mater Trans A Phys Metall Mater Sci 2018;49:5118–36. https://doi.org/10.1007/s11661-018-4826-6.
[176] Chauvet E, Kontis P, Jägle EA, Gault B, Raabe D, Tassin C, Blandin JJ, Dendievel R, Vayre B, Abed S, Martin G. Hot cracking mechanism affecting a non-weldable ni-based superalloy produced by selective electron beam melting. Acta Mater 2018;142:82–94. https://doi.org/10.1016/j.actamat.2017.09.047.
[177] Zhong M, Sun H, Liu W, Zhu X, He J. Boundary liquation and interface cracking characterization in laser deposition of Inconel 738 on directionally solidified ni-based superalloy. Scr Mater 2005;53:159–64. https://doi.org/10.1016/j.scriptamat.2005.03.047.
[178] Vartanian K, Lucas B, Karen M, Cobbs T. Powder Bed Fusion vs Directed Energy Deposition Benchmark Study: Mid-size Part With Simple Geometry. 2021.
[179] Liu R, Wang Z, Sparks T, Liou F, Newkirk J. Aerospace applications of laser additive manufacturing. In: Laser Addit. Manuf. Mater. Des. Technol. Appl. Elsevier Inc.; 2017. p. 351–71. https://doi.org/10.1016/B978-0-08-100433-3.00013-0.
[180] Hauser C. Case Study: Laser Powder Metal Deposition Manufacturing of Complex Real Parts. 2014.
[181] Optomec, Metal 3d Printing Materials - Optomec Additive Manufacturing, (n.d.). https://optomec.com/3d-printed-metals/lens-materials/ (accessed June 24, 2021).
[182] Mori DMG. Lasertec 65 DED Hybrid. 2021.
[183] Meltio, Stainless Steel-SS 316L, n.d. www.meltio3d.com (accessed June 24, 2021).
[184] Meltio, Titanium Alloy-Ti-6Al-4V, n.d. www.meltio3d.com (accessed June 24, 2021).
[185] Liu M, Kumar A, Bukkapatnam S, Kuttolamadom M. A review of the anomalies in directed energy deposition (DED) processes & potential solutions - Part quality & defects. In: Procedia Manuf. Elsevier; 2021. p. 507–18. https://doi.org/10.1016/j.promfg.2021.06.093.
[186] Dass A, Moridi A. State of the art in directed energy deposition: from additive manufacturing to materials design. Coatings 2019;9:418. https://doi.org/10.3390/COATINGS9070418.
[187] Rodrigues TA, Duarte V, Miranda RM, Santos TG, Oliveira JP. Current status and perspectives on wire and arc additive manufacturing (WAAM). Materials (Basel) 2019;12:1121. https://doi.org/10.3390/ma12071121.
[188] Treutler K, Wesling V. The current state of research of wire arc additive manufacturing (Waam): a review. Appl Sci 2021;11. https://doi.org/10.3390/app11188619.
[189] Caiazzo F, Alfieri V, Bolelli G. Residual stress in laser-based directed energy deposition of aluminum alloy 2024: simulation and validation. Int. J. Adv. Manuf. Technol. 2022;118:1197–211. https://doi.org/10.1007/s00170-021-07988-2.
[190] Srivastava S, Garg RK, Sharma VS, Sachdeva A. Measurement and mitigation of residual stress in wire-arc additive manufacturing: a review of macro-scale continuum modelling approach. Arch Comput Methods Eng 2021;28:3491–515. https://doi.org/10.1007/s11831-020-09511-4.
[191] Svetlizky D, Das M, Zheng B, Vyatskikh AL, Bose S, Bandyopadhyay A, Schoenung JM, Lavernia EJ, Eliaz N. Directed energy deposition (DED) additive manufacturing: physical characteristics, defects, challenges and applications. Mater Today 2021;49:271–95. https://doi.org/10.1016/j.mattod.2021.03.020.
[192] Liu P, Yi K, Jeon I, Sohn H. Porosity inspection in directed energy deposition additive manufacturing based on transient thermoreflectance measurement. NDT E Int 2021;122:102491. https://doi.org/10.1016/j.ndteint.2021.102491.
[193] Ahn DG. Directed energy deposition (DED) process: state of the art. Int. J. Precis. Eng. Manuf. Green Technol. 2021;8:703–42. https://doi.org/10.1007/s40684-020-00302-7.
[194] DMG Mori, LASERTEC 6600 DED hybrid, (n.d.). https://uk.dmgmori.com/products/machines/additive-manufacturing/powder-nozzle/lasertec-6600-ded-hybrid (accessed February 8, 2022).
[195] Yamazaki Mazak, VC-500A 5X, (n.d.). https://www.mazakusa.com/machines/vc-500a-5x/ (accessed February 8, 2022).
[196] Romi. Romi D series. https://www.romi.com/en/produtos/romi-d-series/; 2008 (accessed February 8, 2022).
[197] Yang Y, Gong Y, Li C, Wen X, Sun J. Mechanical performance of 316 L stainless steel by hybrid directed energy deposition and thermal milling process. J Mater Process Technol 2021;291:117023. https://doi.org/10.1016/j.jmatprotec.2020.117023.
[198] Feldhausen T, Raghavan N, Saleeby K, Love L, Kurfess T. Mechanical properties and microstructure of 316L stainless steel produced by hybrid manufacturing. J Mater Process Technol 2021;290:116970. https://doi.org/10.1016/j.jmatprotec.2020.116970.
[199] Fu Y, Zhang H, Wang G, Wang H. Investigation of mechanical properties for hybrid deposition and micro-rolling of bainite steel. J Mater Process Technol 2017;250:220–7. https://doi.org/10.1016/j.jmatprotec.2017.07.023.
[200] Duarte VR, Rodrigues TA, Schell N, Miranda RM, Oliveira JP, Santos TG. Hot forging wire and arc additive manufacturing (HF-WAAM). Addit Manuf 2020;35:101193. https://doi.org/10.1016/j.addma.2020.101193.
[201] Bambach M, Sizova I, Sydow B, Hemes S, Meiners F. Hybrid manufacturing of components from Ti-6Al-4V by metal forming and wire-arc additive manufacturing. J Mater Process Technol 2020;282:116689. https://doi.org/10.1016/j.jmatprotec.2020.116689.
[202] Hemes S, Meiners F, Sizova I, Hama-Saleh R, Röhrens D, Weisheit A, Häfner CL, Bambach M. Microstructures and mechanical properties of hybrid, addi-tively manufactured ti6al4v after thermomechanical processing. Materials (Basel) 2021;14:1–14. https://doi.org/10.3390/ma14041039.
[203] Xu X, Ganguly S, Ding J, Seow CE, Williams S. Enhancing mechanical properties of wire + arc additively manufactured INCONEL 718 superalloy through in-process thermomechanical processing. Mater Des 2018;160:1042–51. https://doi.org/10.1016/j.matdes.2018.10.038.
[204] Gu J, Wang X, Bai J, Ding J, Williams S, Zhai Y, Liu K. Deformation microstructures and strengthening mechanisms for the wire+arc additively manufactured Al-Mg4.5Mn alloy with inter-layer rolling. Mater Sci Eng A 2018;712:292–301. https://doi.org/10.1016/j.msea.2017.11.113.
[205] Sefene EM, Hailu YM, Tsegaw AA. Metal hybrid additive manufacturing: state-of-the-art. Prog Addit Manuf 2022. https://doi.org/10.1007/s40964-022-00262-1.
[206] Dilberoglu UM, Gharehpapagh B, Yaman U, Dolen M. The role of additive manufacturing in the era of industry 4.0. Procedia Manuf 2017;11:545–54. https://doi.org/10.1016/j.promfg.2017.07.148.
[207] Cortina M, Arrizubieta JI, Lamikiz A, Ukar E. Impact of cutting fluid on hybrid manufacturing of AISI H13 tool steel. Rapid Prototyp. J. 2021. https://doi.org/10.1108/rpj-04-2021-0073. ahead-of-p.
[208] Williams SW, Martina F, Addison AC, Ding J, Pardal G, Colegrove P. Wire + Arc additive manufacturing. Mater Sci Technol (UK) 2016;32:641–7. https://doi.org/10.1179/1743284715Y.0000000073.
[209] Dass A, Moridi A. State of the art in directed energy deposition: from additive manufacturing to materials design. Coatings 2019;9. https://doi.org/10.3390/COATINGS9070418.
[210] Gao C, Wolff S, Wang S. Eco-friendly additive manufacturing of metals: Energy efficiency and life cycle analysis. J Manuf Syst 2021;60:459–72. https://doi.org/10.1016/j.jmsy.2021.06.011.
[211] World Steel Association. In: Climate change and the production of iron and steel. World Steel Assoc.; 2021. p. 8 (accessed August 7, 2021), https://www.steel.org.au/resources/elibrary/resource-items/steel-s-contribution-to-a-low-carbon-future-and-cl/.
[212] United Nations Environment Programme. Emissions gap report. 2015.
[213] International Energy Agency. Global CO2 emissions in 2019 analysis. https://www.iea.org/articles/global-co2-emissions-in-2019; 2020 (accessed September 9, 2021).
[214] World Economic Forum (WEC). Aluminium for Climate : Exploring pathways to decarbonize the aluminium industry. https://www3.weforum.org/docs/WEF_Aluminium_for_Climate_2020.pdf; 2020.
[215] Huang MT, Zhai PM. Achieving Paris Agreement temperature goals requires carbon neutrality by middle century with far-reaching transitions in the whole society. Adv Clim Chang Res 2021;12:281–6. https://doi.org/10.1016/j.accre.2021.03.004.
[216] Ahn DG. Direct metal additive manufacturing processes and their sustainable applications for green technology: a review. Int J Precis Eng Manuf Green Technol 2016;3:381–95. https://doi.org/10.1007/s40684-016-0048-9.
[217] Tomlin M, Meyer J, , J.M.-P of the 7th A.C. Technology U., Meyer J. In: Topology optimization of an additive layer manufactured (ALM) aerospace part, 7th Altair CAE Technol. Conf. 2011; 2011. p. 1–9.

[218] Huang R, Riddle M, Graziano D, Warren J, Das S, Nimbalkar S, Cresko J, Masanet E. Energy and emissions saving potential of additive manufacturing: the case of lightweight aircraft components. J Clean Prod 2016;135:1559–70. https://doi.org/10.1016/j.jclepro.2015.04.109.
[219] Son D, Kim S, Jeong B. Sustainable part consolidation model for customized products in closed-loop supply chain with additive manufacturing hub. Addit Manuf 2021;37:101643. https://doi.org/10.1016/j.addma.2020.101643.
[220] Yang S, Talekar T, Sulthan MA, Zhao YF. A generic sustainability assessment model towards consolidated parts fabricated by additive manufacturing process. In: Procedia Manuf. Elsevier B.V.; 2017. p. 831–44. https://doi.org/10.1016/j.promfg.2017.07.086.
[221] Kellens K, Baumers M, Gutowski TG, Flanagan W, Lifset R, Duflou JR. Environmental dimensions of additive manufacturing: mapping application domains and their environmental implications. J Ind Ecol 2017;21:S49–68. https://doi.org/10.1111/jiec.12629.
[222] Bennett J, Garcia D, Kendrick M, Hartman T, Hyatt G, Ehmann K, You F, Cao J. Repairing automotive dies with directed energy deposition: industrial application and life cycle analysis. J Manuf Sci Eng Trans ASME 2019;141. https://doi.org/10.1115/1.4042078.
[223] Agrawal R, Vinodh S. State of art review on sustainable additive manufacturing. Rapid Prototyp J 2019;25:1045–60. https://doi.org/10.1108/RPJ-04-2018-0085/FULL/PDF.
[224] Yilmaz TG, Tüfekçi M, Karpat F. A study of lightweight door hinges of commercial vehicles using aluminum instead of steel for sustainable transportation. Sustain 2017;9. https://doi.org/10.3390/su9101661.
[225] Spreafico C. Can modified components make cars greener? A life cycle assessment. J Clean Prod 2021;307:127190. https://doi.org/10.1016/j.jclepro.2021.127190.
[226] Salonitis K. Energy efficiency of metallic powder bed additive manufacturing processes. In: Environ. Footprints Eco-Design Prod. Process. Springer; 2016. p. 1–29. https://doi.org/10.1007/978-981-10-0606-7_1.
[227] Ribeiro I, Matos F, Jacinto C, Salman H, Cardeal G, Carvalho H, Godina R, Peças P. Framework for life cycle sustainability assessment of additive manufacturing. Sustain 2020;12:929. https://doi.org/10.3390/su12030929.
[228] Bekker ACM, Verlinden JC. Life cycle assessment of wire + arc additive manufacturing compared to green sand casting and CNC milling in stainless steel. J Clean Prod 2018;177:438–47. https://doi.org/10.1016/j.jclepro.2017.12.148.
[229] M. Armstrong, H. Mehrabi, N. Naveed, Environmental Impact of Metal Additive Manufacturing, n.d.
[230] Faludi J, Hu Z, Alrashed S, Braunholz C, Kaul S, Kassaye L. Does material choice drive sustainability of 3D printing? Int J Mech Aerospace Ind Mechatronics Eng 2015;9:144–51.
[231] Baumers M, Tuck C, Wildman R, Ashcroft I, Hague R. Energy inputs to additive manufacturing: does capacity utilization matter?. In: 22nd Annu. Int. Solid Free. Fabr. Symp. - An Addit. Manuf. Conf. SFF 2011; 2011. p. 30–40.
[232] Peng T, Kellens K, Tang R, Chen C, Chen G. Sustainability of additive manufacturing: An overview on its energy demand and environmental impact. Addit Manuf 2018;21:694–704. https://doi.org/10.1016/j.addma.2018.04.022.
[233] Ahsan A, Ali M, Ali HM, Qadeer MA, Khan SA. Implementation analysis of ISO 50001: 2011 energy management system (EnMS) on a small/medium enterprise. Tech J 2016;20:8.
[234] Rosenqvist J, Thollander P, Rohdin P, Sderstrm M. Industrial energy auditing for increased sustainability – methodology and measurements. In: Sustain. Energy - Recent Stud. InTech; 2012. https://doi.org/10.5772/51717 (accessed May 19, 2021).
[235] Haraldsson J, Johansson MT. Barriers to and drivers for improved energy efficiency in the Swedish aluminium industry and aluminium casting foundries. Sustain 2019;11:2043. https://doi.org/10.3390/su11072043.
[236] Salonitis K, Zeng B, Mehrabi HA, Jolly M. The challenges for energy efficient casting processes. In: Procedia CIRP. Elsevier; 2016. p. 24–9. https://doi.org/10.1016/j.procir.2016.01.043.